Assessment of graphene oxide ecotoxicity at several trophic levels using aquatic microcosms

Lauris Evariste, Antoine Mottier, Laura Lagier, Stéphanie Cadarsi, Maialen Barret, Cyril Sarrieu, Brigitte Soula, Florence Mouchet, Emmanuel Flahaut, Cécile Cels-Pinelli, et al.

Assessment of graphene oxide ecotoxicity at several trophic levels using aquatic microcosms

Lauris Evariste [a], Antoine Mottier [a], Laura Lagier [a], Stéphanie Cadarsi [a], Maialen Barret [a], Cyril Sarrieu [b], Brigitte Soula [b], Florence Mouchet [a,*], Emmanuel Flahaut [b], Eric Pinelli [a], Laury Gauthier [a]

[a] EcoLab, Université de Toulouse, CNRS, INPT, UPS, Toulouse, France
[b] CIRIMAT, Université de Toulouse, CNRS, INPT, UPS, UMR CNRS-UPS-INP N° 5085, Université Toulouse 3 Paul Sabatier, Bât. CIRIMAT, 118 route de Narbonne, 31062, Toulouse cedex 9, France

A B S T R A C T

Extensive development of new applications using graphene based materials such as graphene oxide (GO) increases its potential release and occurrence into aquatic environments, raising the question of its biological and ecological risks. As standardized single species based assays fail to highlight toxicological pathways implying interactions between organisms, the use of micro/mesocosms appears as a good solution to fill the lack of environmental realism inherent to these tests. In this work, experiments were achieved using microcosm systems to expose a reconstituted food chain to GO at environmentally relevant concentrations (0.05 and 0.1 mg L^{-1}). The trophic chain was composed of a consortium of algae and bacteria as primary producers, chironomid larvae as primary consumers and decomposers while larvae of the amphibian *Pleurodeles waltii* constituted the secondary consumers. Monitoring of multiple ecotoxicological and ecological endpoints allowed to observe changes in bacterial communities while no toxic effects were noticed in chironomids. However, chironomids feeding behaviour changed as a consequence of GO contamination, leading to an increase in leaf litter consumption. Genotoxic effects were noticed in *Pleurodeles* larvae. This study highlights the importance of using such experimental systems to better encompass the ecotoxic potential of GO through the determination of toxicological routes and consequences on ecosystem's functioning.

1. Introduction

Carbon based nanoparticles (CBNs) possess unique properties (high surface area, electrical and thermal conductivity, mechanical strength and optical transmittance) triggering tremendous scientific expectations for development of a wide range of industrial applications [1–5]. Graphene oxide (GO) is a chemically oxidized form of graphene that consists of a single atom thick two dimensional sheet of carbon atoms containing epoxide, hydroxyl and carboxyl groups. Due to its high oxygen content, GO is a hydrophilic nanomaterial that is stable when dispersed in aqueous media [6]. As other engineered nanoparticles (ENPs), GO is likely to be released into the ecosystems at any stage of its life cycle, from the production, the uses and the waste treatments of the substance and may cause environmental and health issues [7–10]. Due to its hydrophilic properties associated to high surface area and chemical functions, GO could potentially react with many components of the environment, modifying its ecological risk toward aquatic ecosystems [11].

Numerous toxicological studies of graphene based nanomaterials (GBNs) were performed on mammalian cell lines or human related biological models [8,12–14] while potential effects on environmentally relevant models were not sufficiently investigated [15,16]. In addition, existing studies used assays performed through exposure of single species to CBNs are essential to understand toxicological mechanisms, these tests are poorly representative of environmental conditions [17]. For this purpose, the use of more complex systems such as micro mesocosms was shown to be efficient to assess the ecotoxic potential of multiple contaminants under environmentally relevant conditions [17–20]. These experimental systems allow measurement of both

* Corresponding author.
E-mail address: florence.mouchet@ensat.fr (F. Mouchet).

https://doi.org/10.1016/j.carbon.2019.09.051

ecosystemic and toxicological endpoints in multiple interacting species or communities, from different trophic levels, after direct exposure of organisms as well as through trophic routes [21–23]. Thus, performing this type of study is becoming crucial for a better understanding of potential environmental issues implying any contaminant and including GO.

Previous works mainly focused on the ecotoxicological effects of GO on organisms from lower trophic levels such as bacteria or algae exposed in single culture. Antibacterial activity of GO was identified [24–26] and among multiple GBNs, GO was shown to exert the highest cytotoxicity toward the bacterial model *Escherichia coli* [27]. Concerning adverse effects toward algae, it was demonstrated that GO exposure led to *Chlorella* sp. growth inhibition and produced membrane damages through mechanical actions as well as oxidative stress induction [28,29]. Studies carried out on organisms from higher trophic levels (*i.e.* primary and secondary consumers) are still scarce. It was indicated that GO induced behavioral disturbances of crustacean larvae (*Amphibalanus amphitrite* and *Artemia salina*) and was strongly accumulated in digestive tract [30,31]. In amphibians, similar accumulation of GO was observed in gut of *Xenopus laevis* tadpoles and growth was inhibited at high concentrations [32]. Observation of toxicological effects induced by GO on low trophic level organisms raises the question of possible larger scale conse quences through trophic network and on ecosystem functioning.

The aim of this study was to investigate the toxicity of GO under realistic conditions to go further in the understanding of its impact on organisms occupying multiple trophic levels and to determine potential consequences on ecosystem's functioning. For this pur pose, microcosm systems were used to expose organisms interacting through a reconstituted trophic chain. The biological models retained for the study were chosen for being key species represen tative of a simplified trophic chain from pond ecosystems [33,34]. Although they have significant ecological functions, number of hu man activities are threatening these ecosystems as well as the biodiversity they host, especially endangering species such as am phibians [35]. For this purpose, the benthic diatom *Nitzschia palea* and a bacterial consortium were settled to form a biofilm providing food for chironomid larvae (*Chironomus riparius*) as primary con sumers and decomposers. Secondary consumers were constituted by the carnivorous larvae of the amphibian, *Pleurodeles waltl*, the Spanish newt, that feed on macro invertebrates. As microbial com munities are at the very basis of every ecosystem functioning and due to their implication on global nutrient cycling [36], changes in microorganism community composition were monitored during the experiment. In terms of toxicological endpoints, survival and growth parameters of the consumers were controlled as well as morpho logical deformities in chironomids and count of micronucleated erythrocytes in *Pleurodeles* [37,38]. Analysis of chironomids mouth part deformities constitutes a marker of teratogenesis that is widely used in pollution monitoring as well as micronuclei induction that is a good indicator of genotoxicity, integrating aneugenic and clasto genic effects that is used as endpoint in ISO 21427–1 procedure. Both teratogenic and genotoxic biomarkers are considered as highly predictable ecological endpoints at the population, community and ecosystem level [39]. The process of leaf litter decomposition ensured by chironomids and bacteria was also investigated, as it constitutes an interesting functional ecological marker integrative of lower trophic level activities [22,40].

2. Material and method

2.1. Graphene oxide nanoparticles

Graphene oxide nanoparticles were produced from twisted ribbon shaped carbon nanofibers (GANF®) processed by Hummer method [41] and supplied by Antolin Group. Full characterization of the tested material was already presented in earlier work [42] and data are summarized in Table 1. Both experiments were performed within few weeks. GO was stored as dry powder in the dark and dispersions were prepared extemporaneously in order to avoid any possible change of material characteristics.

2.2. Stability of graphene oxide suspension in exposure media

The stability of the suspension of GO was evaluated using a Turbiscan LAB (Formulation) equipment, at room temperature. Suspensions were prepared at 10 mg L^{-1} in deionised water (EDI) or Volvic water immediately before analysis. This concentration was assessed as low GO concentrations low could not be detected by TurbiscanTM. The suspension was bath sonicated for 2 min before insertion into the measurement chamber. Sedimentation was monitored for 24 h with 1 scan per minute by measuring during each scan the transmission of the suspension vs the height in the vial. In case of sedimentation, it is thus expected that the transmission will increase at the heights where particles have settled down, while it should decrease where sedimented particles are present.

2.3. Microcosm exposure

Nine microcosms (glass tanks 60 × 30 × 30 cm, L x W x H) were filled with 6780 g of reconstituted sediment: (96.6% of silica sand, 2.4% of kaolinite and 1% of $CaCO_3$) and 40 L of the commercial natural spring water Volvic® (Ca^{2+}: 12 mg L^{-1}, Na^{+}: 12 mg L^{-1} Mg^{2+}: 8 mg L^{-1}, K^{+}: 6 mg L^{-1}, Cl^{-}: 1 mg L^{-1} and Si: 32 mg L^{-1}) as used in previous microcosm studies [21,43–45]. In order to maintain correct oxygenation, each tank was equipped with a recirculation system. Light was provided by fluorescent tubes (JBL solar ultra, Natur 9000°K LT 24 WT5 HQ) and photope riod was set on 12:12 light/night. Temperature (21.5 ± 0.9 °C), conductivity (234.3 ± 9.1 µS cm^{-1}), pH (7.9 ± 0.4), redox potential (306.6 ± 17.3 mV) and dissolved oxygen (9.1 ± 1.2 mg L^{-1}) were monitored continuously (Ponsel Odeon open X probes kit). Nitro gen products (NO_3^-, NO_2^- and NH_4^+) were monitored twice a week using a HI83203 photometer (Hanna instruments) and dissolved organic carbon was measured at each sampling time by infrared detection of CO_2 produced by catalytic oxidation at 680 °C (Table S1).

Three different exposure conditions were tested: control (nat ural spring water), graphene oxide at the final concentration of 0.05 mg L^{-1} and graphene oxide at the final concentration of 0.1 mg L^{-1}. Each condition was tested in triplicate with random assignation of the microcosms. Contamination of the microcosms

Table 1
Physico-chemical characteristics of GO used for the experiment. at. %: atomic %; Csp2: sp^2 carbon; Sat.: shake-up satellites (π to π^* transitions); TEM: transmission electron microscope; HRTEM: high resolution TEM; BET: Brunauer-Emett-Teller.

	Graphene Oxide
Carbon content	69.0 at. %
Oxygen content	31.0 at. %
Csp2 graphene	35.5 at. %
C OH/C O C	24.7 at. %
C O	2.5 at. %
O C O	5.3 at. %
Sat.	1.4 at. %
Number of layers (HRTEM)	1 5
Lateral size (TEM)	0.2 8 µm
Specific surface area (BET)	228 ± 7 m^2 g^{-1}

by graphene oxide nanoparticles was performed sequentially through the addition of 1/12^{e} of the final concentration over 10 days to reach the final concentration indicated by the condition name (0.05 mg L^{-1} and 0.1 mg L^{-1}) (Fig. 1).

The progress of the experiment and the order in which the different organisms were introduced are shown in Fig. 1. Senescent alder leaves (*Alnus glutinosa Gaertn.*) (3.2 g dry mass/mesocosm) were added the first week for measurement of decomposition rate and microorganisms (microbial consortium 1×10^6 cells/ml and *Nitzschia palea* 2.05×10^4 cells/ml) were allowed to settle and develop during 3 weeks without any contamination. This duration was necessary for the development of the primary producers leading to the formation of a biofilm covering the whole sediment [44] and equilibration of nitrogen products in the microcosms by bacteria. The first samplings of the biofilm and water were per formed to analyse microorganism communities prior to contami nation and addition of primary and secondary consumers (T0). Other organisms, bred in the laboratory facilities, were added sequentially to the microcosms (Fig. 1). 800 *Chironomus riparius* individuals aged of 72 h and 15 *Pleurodeles waltii* individuals at stage 53 of development [46] were added during the fourth week to allow an exposure duration of 13 and 10 days respectively. These durations were chosen in order to ensure that the surviving *C. riparius* would develop until the stage 4 (required condition for teratogenicity analysis). Moreover, chironomids were added prior to the newts to grow and start to accumulate GO in order to ensure trophic transfer towards the secondary consumers. For *Pleurodeles*, exposure duration of 10 days is necessary for genotoxic assessment at low dose [47]. A second sampling of the microorganisms was performed when half of the final GO dose was reached (T1) and at the end of the exposure when the full dose was reached (T2). *Xenopus laevis* (n 40) at stage 50 of development [48] were added during the week 5 as a food complement for *Pleurodeles* larvae. Chironomids, *Pleurodeles* and alder leaves were also sampled at T2, constituting the end of the experiment.

2.4. Endpoint measurement

2.4.1. Primary compartment: sampling, DNA extraction, PCR and sequencing

Water and sediment were sampled at 3 different times during the experiment (T0, T1 and T2). At each sampling time, 100 mL of water and 10 mL of sediment were taken. Water samples were filtered on a 5 μm filter (Whatman® Nuclepore™ Track Etched Membranes) in order to recover microorganisms from the water column. Filters and sediment samples were snap frozen in liquid nitrogen and stored at 80 °C before processing for analyses. Total DNA was extracted from water samples and sediment subsamples (644.6 ± 37.2 mg) using the Mobio® power soil DNA isolation kit following manufacturer's instructions. Additionally, negative extraction controls were performed to ensure the absence of DNA contamination during the process. The quantity and quality of DNA extracts was analysed using a NanoDrop 2000 UV spectropho tometer (Thermo Scientific).

The V4–V5 region of *archeae* and bacteria 16S rRNA gene was targeted using PCR1_515F (5′ GTGYCAGCMGCCGCGGTA 3′) and PCR1_928R (5′ CCCCGYCAATTCMTTTRAGT 3′) primers set [49]. PCRs were performed on a Gene AmpTM PCR system 9700 ther mocycler (Applied Biosystems, Forster City, CA, United States) in a final volume of 50 μL containing: 37.5 μL of PCR water, 5 μL of 10X PCR buffer, 2 μL of extracted DNA, 2 μL of both primer (10 μM), 1 μL of dNTP (2.5 mM) and 0.5 μL of Taq DNA polymerase (5 U/μL – Sigma Aldrich). The following PCR protocol was applied: 94 °C for 120 s, 30 cycles of 94 °C for 60 s, 65 °C for 40 s, 72 °C 30 s and 72 °C for 10 min.

Sequencing of amplicons from 16S rRNA genes was performed using Illumina MiSeq technology (2 × 250 pb) by the Get_PlaGe platform (Genotoul, Toulouse, France). Bioinformatic analysis was performed using FROGS (Find Rapidly Operational Taxonomic Units (OTU) Galaxy Solution) pipeline on Galaxy [50]. Briefly, sequences with mismatches in the primers were excluded and PCR primers were trimmed. Reads were clustered into OTUs using the Swarm clustering method [51]. Chimera were removed and filters were applied to keep OTUs present in at least 3 samples and representing at least 0.005% of all sequences [52]. 478 OTUs were assigned at different taxonomic levels (from Kingdom to species) using RDP classifier and NCBI Blast + on Silva 132 database (pintail 80) [53].

2.4.2. Chironomids

At the end of the experiment, mortality, growth and teratoge nicity were assessed in chironomid larvae that were not predated by Pleurodeles. A careful sorting of the sediment allowed to count the surviving individuals which were then measured using the image J software (total length and width of the cephalic capsule).

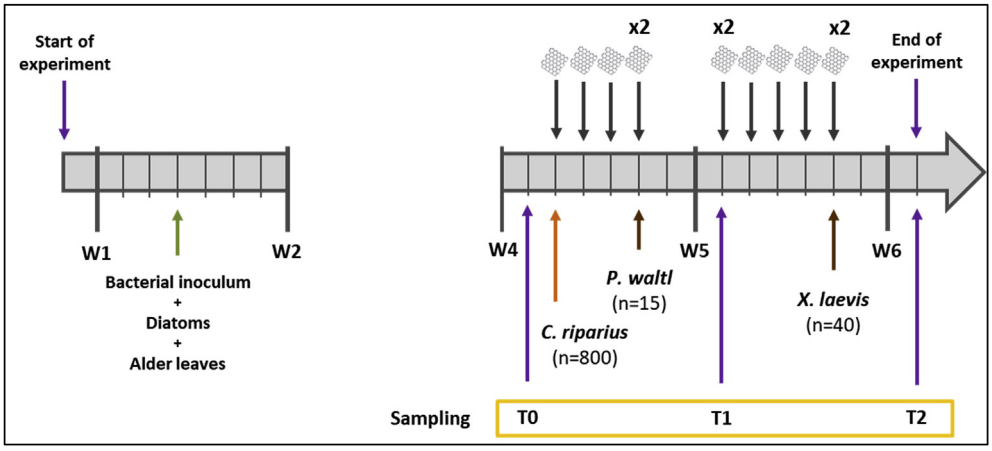

Fig. 1. Scheme of the time-progress of the microcosm experiment. Bacterial consortium and diatoms were allowed to settle and develop to colonize the sediment and alder leaves during 3 weeks. Prior to the addition of other organisms and GO, a first sampling of the primary compartment was performed (T0). GO was then added sequentially in the microcosms over 2 weeks to reach 0.05 mg L ^{1} and 0.1 mg L ^{1} as final concentration. Pleurodeles (*P. waltl*) and Chironomids (*C. riparius*) were added subsequently during the fourth week while a second sampling of microbial consortium was performed at the end of that same week (T1). All organisms were sampled at the beginning of the 6th week to perform analysis of the different endpoints (T2). (A colour version of this figure can be viewed online.)

The cephalic capsules were recovered and discolored in potassium hydroxide (15%, 95 °C, 15 min), then mounted on microscope slides with quick hardening medium (Sigma). Teratogenecity was assessed by counting the number of deformities in mentum. Ac cording to Salmelin et al. [38], only absolute deformities such as missing and extra teeth and Kohn gaps were taken into account.

2.4.3. Leaf litter degradation

Alder leaves degradation was estimated by the total surface of degradation after microcosm exposure. Leaves were scanned at the beginning and at the end of experiment using a flatbed scanner with 600 DPI resolution. Leaves pictures were processed with image J software: a 8 bit transformation and thresholding allowed us to quantify the degraded surfaces.

2.4.4. Amphibians

No endpoint was measured in *X. laevis* tadpoles that were all predated during the experiment by *Pleurodeles* larvae. For *Pleuro deles* larvae, mortality, growth and genotoxicity were studied after 10 days of exposure (n 15 for each endpoint per microcosm). Mortality was checked daily throughout the exposure. Growth was studied by measurements of size (photo and image analysis with Image J software) at the beginning and end of the experiment. Genotoxicity was assessed by enumeration of micronucleated erythrocytes (MNE) in blood smears after fixation (methanol 99.9%) and staining (groat hematoxylin). The number of cells containing one or more micronuclei was counted among a total of 1000 cells.

2.5. Statistical analysis

Statistical analysis was performed using Minitab 16 Statistical software. Data of growth (*P. waltl* and *C. riparius*), development and survival chironomids (growth, development and survival) as well as leaf litter degradation endpoints were analysed using one way ANOVA when assumptions of normality and homogeneity of vari ance were met. As it was not the case for genotoxicity data, non parametric Kruskal Wallis followed by Dunn's multiple compari son test was performed. For metagenomics analysis, data manip ulations, OTUs counts, alpha diversity indexes and Unifrac Distances calculations as well as multidimensional scaling (MDS) plot were carried out using "Phyloseq" R package [54]. Differential abundance of bacterial genera between exposed conditions compared to the control group was examined using "Deseq2" R package [55]. PERMANOVA was performed using Adonis function from the "vegan" R package [56]. The relationships between the biological responses measured were explored by multivariate Principal Component Analysis (PCA) and correlation analyses using "ade4 R" package [57].

3. Results

3.1. Behaviour of GO in exposure media

The variation of the transmission data (compared to t0) vs time for EDI and Volvic are presented in Fig. 2. While the dispersion is stable over 24 h in EDI medium, a clear homogeneous sedimenta tion is evidenced in the case of the Volvic water after 5 h (Fig. S1).

3.2. Effects on lower trophic level

Bacterial communities in water compartment were different from those in sediment compartment regardless of time and GO concentration, as revealed by MDS and PERMANOVA analysis using unweighted UniFrac distances (Fig. S2) (F 32.554; r^2 0.385; p 0.001). Thus, the two compartments were studied separately to analyse the effects occurring on compartment associated bacterial communities. At T0, prior to contamination, community structures in the water were similar between the condition related micro cosms (PERMANOVA: F 1.193; r^2 0.284; p 0.132), and the same was observed in sediments (F 1.143; r^2 0.276; p 0.252).

3.2.1. Effects on microorganisms from the water column

When analysing the alpha diversity, no difference was measured for the observed diversity, Chao1 and Shannon indexes in the water column, during the whole experiment (Fig. S3A). However, exposure duration as well as GO concentration were shown to significantly affect the microbial community structure (PERMANOVA: Contami nant: F 1.657; r^2 0.104; p 0.010; Exposure duration: F 3.428; r^2 0.216; p 0.001). MDS analysis indicated a higher contribution of the exposure duration (first axis) toward bacterial community composition compared to GO concentration (second axis) (Fig. S3B). In the water column at T0, over 95% of overall community was represented by phyla Proteobacteria and Bacteroidetes with a rela tive abundance of $58.8 \pm 21.6\%$ and $37.5 \pm 22.2\%$ respectively (Fig. 3A). The relative abundance of none of the phyla analysed was shown to be impacted by GO contamination (Table S2). Focusing on families from the two main phyla found in the water column (Fig. S4), almost no effects were observed on relative abundances (Table S2). Analysis of the genera differential abundance in the GO conditions compared to the control group during the overall expo sure led to a significant decrease of 3 genera from the phylum Pro teobacteria (*Legionella*, *Sphingobium* and *Reyranella*) when exposed to 0.05 mg L^{-1} of GO, while three other genera from this phylum were decreased in the 0.1 mg L^{-1} exposure condition (*Pseudomino bacter*, *Sphingorhabdus* and *Devosia*) (Fig. S5A).

3.2.2. Effects on microorganisms in sediment

A significant increase in the biofilm observed richness and Chao1 was noticed between T0 and T1 without being influenced by GO concentration and remained stable until T2 while values of the Shannon index were not significantly influenced (Fig. 4A). Exposure duration and GO concentration significantly affected microbial community structure (PERMANOVA: Contaminant: F 2.862; r^2 0.161; p 0.002, Exposure duration: F 4.875; r^2 0.274; p 0.001) with a greater contribution of the exposure duration over the contaminant concentration (Fig. 4B). At T0, prior to contamination by GO, three main phyla constituted the bacterial compartment of the biofilm. Phyla Proteobacteria, Bacteroidetes and Planctomycetes relative abundances were of $29.1 \pm 15.1\%$, $10.6 \pm 4.2\%$ and $3.8 \pm 2\%$ respectively. The chloroplastic 16S rRNA gene from diatoms was affiliated to Ochrophyta phylum. This phylum represented $48.7 \pm 20.4\%$ of the overall biofilm organisms (Fig. 3B). The relative abundance of the two main bacterial phyla and diatoms was not affected by exposure to GO, while the phyla Planctomycetes, Armatimonadetes and WPS 2 significantly increased in the presence of GO at 0.1 mg L^{-1} compared to the control group (Table S3). The effects occurring at the family scale in the three main bacterial phyla from the sediment were analysed (see supplementary data and Fig. S6). Analysis of the OTUs differ ential abundances in the biofilm indicated that among 517 OTUs, exposure to GO at 0.05 mg L^{-1} led to significant changes in the relative abundance of 15 taxa, among which 5 were found in a higher abundance and 10 in a lower abundance (Fig. S5B). At 0.1 mg L^{-1}, 20 taxa were differentially abundant compared to the control with an equal distribution between over and under repre sented taxa. The relative abundance of genera *Gemmata*, *Azospir illum* and *Flavobacterium* were shown to decrease in a similar manner in the two GO conditions compared to the control group while genera *Planctopirus* and *Armatimonas* increased in the same order of manitude.

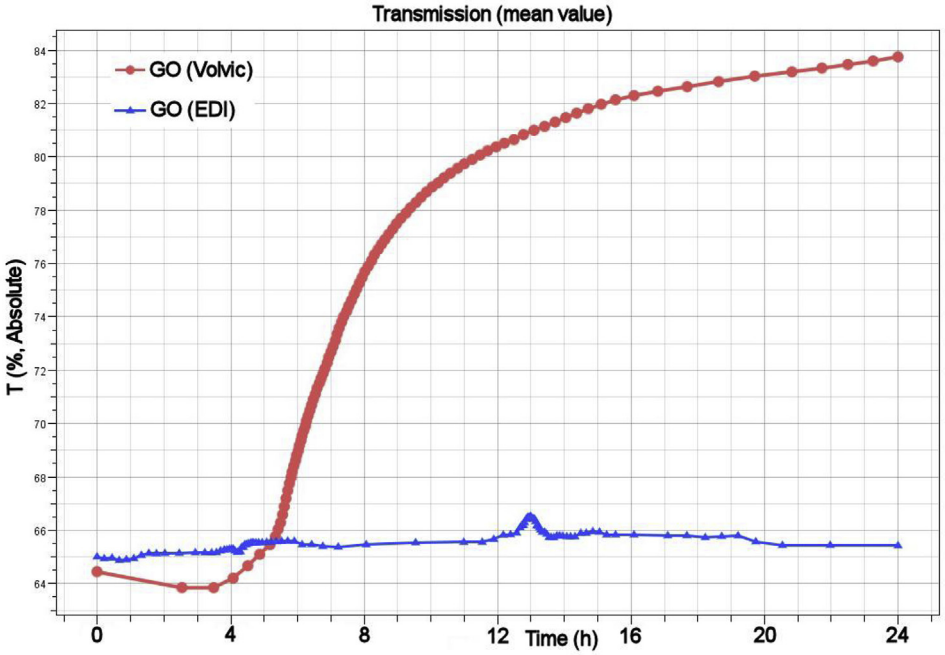

Fig. 2. Variation of the transmission vs time for suspensions of GO at 10 mg L ^{1} in deionised water (blue) or Volvic water (red). (A colour version of this figure can be viewed online.)

3.3. Effects on chironomids

At the end of the experiment, no significant difference was noticed on the survival rate of *C. riparius* whatever the exposure condition (ANOVA, p 0.976). A mean of 8.02 ± 4.7% of the overall chironomids were remaining for all conditions. Larval growth and determination of development stage measured from length of the organisms and head width measurement respectively, were not significantly affected by GO exposure (ANOVA, p 0.280 and 0.860 respectively). Considering the whole organisms, 60.6% of the larvae reached the stage 4 at the end of the experiment and a mean size of 8.6 ± 2.1 mm was measured. Analysis of teratogenicity in stage 4 larvae indicated no effect of GO exposure (ANOVA, p 0.913).

3.4. Effects on leaf litter degradation

At the end of the exposure, a significant increase in leaf degradation was noticed after exposure to 0.05 mg L^{-1} of GO compared to the control group while only a trend in increase of degradation was observed at 0.1 mg L^{-1} (ANOVA p 0.027 followed by Tuckey) (Fig. 5).

3.5. Effects on pleurodeles larvae

No mortality in Pleurodeles larvae was observed during the whole experiment and larval growth was not affected by GO exposure (ANOVA, p 0.723). At the end of the experiment, a significant increase in micronucleated erythrocytes was observed in larvae exposed to 0.1 mg L^{-1} (Kruskal Wallis: p 0.0013 followed by Dunn's test) (Fig. 6).

3.6. Principal component analysis

In the principal component analysis of the responses measured at the different trophic levels, PC1 and PC2 explained 38,6% and 24.3% of the total variance respectively (Fig. 7). The PCA showed a better segregation between the controls microcosms and those contaminated with GO along the PC2 axis based on biological responses. The parameters related to chironomids development and survival as well as microbial diversity were negatively associated with PC1 while teratogenesis was positively associated with PC1. The leaf litter degradation and genotoxicity in pleurodeles were mainly associated with the conditions of GO exposure along PC2.

4. Discussion

To our knowledge, this study is the first one to investigate the effect of GO under environmentally relevant conditions using a reconstituted trophic chain through the use of microcosms. Because of the limited available techniques to quantify GO in complex matrix and changes of materials characteristics over time at environmentally realistic concentrations [58], no relevant quantification analysis could be performed in our study. Thus, the hypothesis of material distribution in our system and toxicological mechanisms involved are based only on Turbiscan data and biological responses measured.

4.1. Behaviour of GO in exposure media

The fate, transport, and bioavailability of GO are mainly determined by their behaviour in aquatic ecosystems including aggregation deposition that can be influenced by multiple factors [66]. On the one hand, interactions with organic matter of the experimental system would increase the colloidal stability of the GO [11,67,68], while on the other hand, the presence of ions in the water such as Ca^{2+} or Na^{+} could adsorb on the negatively charged functional groups of GO, leading to reduced surface charge and reduced dispersion stability, leading to its deposition [69]. According to the obtained results it seems that the interactions with ions of the exposure media occurring under the experimental conditions are responsible for the sedimentation of the GO. Such sedimentation of the material would decrease its bioavailability for organisms from the water column while it will increase for organisms living at the sediment water interface.

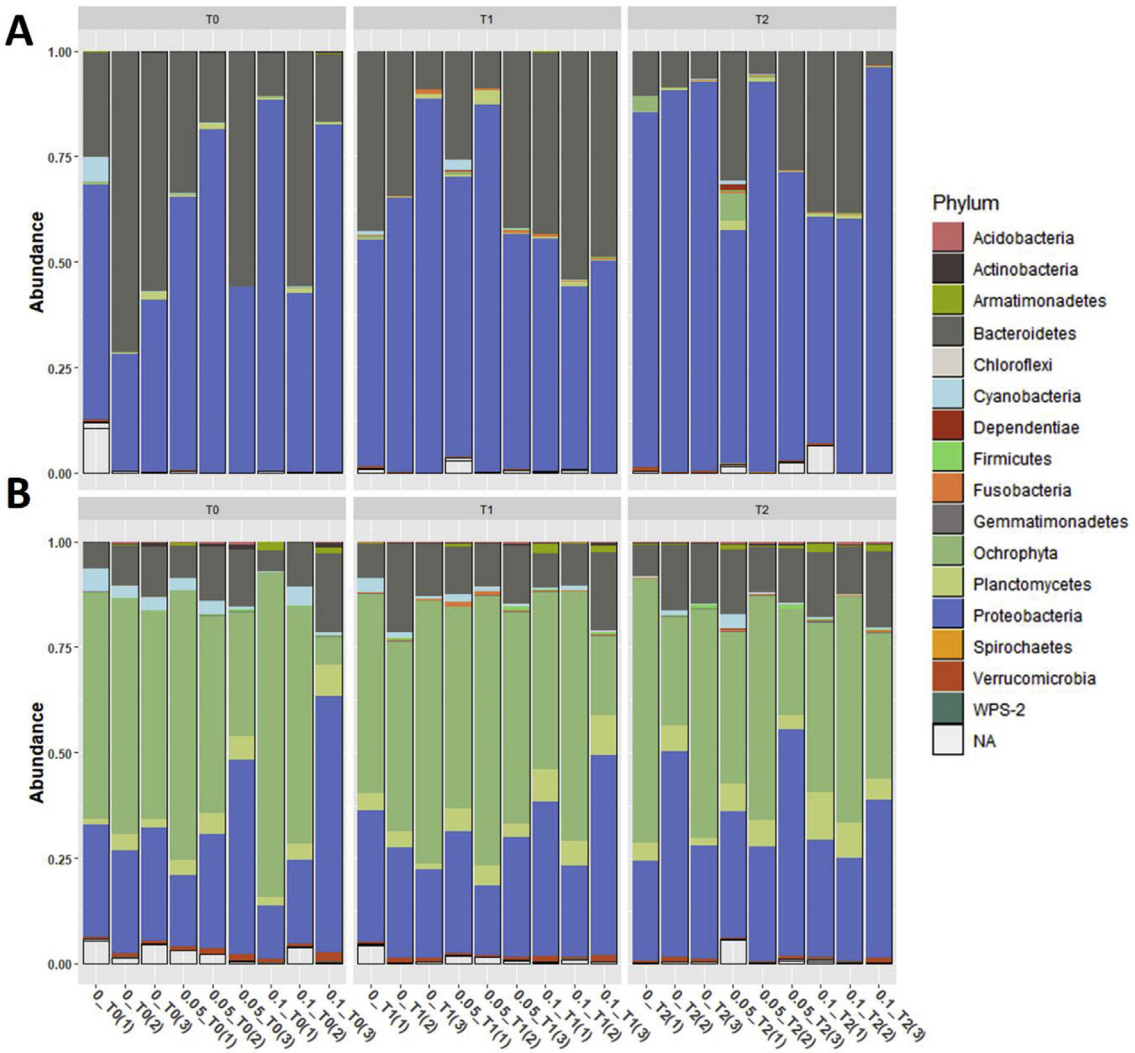

Fig. 3. Relative abundance of bacterial phyla from the water column (A) and in the biofilm of the sediment (B) in function of GO concentration (0, 0.05 and 0.1 mg L^{-1}). (A colour version of this figure can be viewed online.)

4.2. *Effects on microorganisms*

Studying the effects of GO on microorganisms is essential as they constitute the first link of the food chain. Literature is furnished of data demonstrating the antibacterial capacities of GO [24–26,59–61]. However, few studies focused on the effects generated by CBNs on complex bacterial communities from aquatic ecosystems and the data available were mainly obtained on bacterial consortium from soils [62,63] or activated sludge [64,65]. In the present study, complex changes were observed in the bacterial compartment over the whole experiment. It is interesting to point out that GO exposure induced only minor differences in bacterial communities in the water column whereas the biofilm communities were more impacted. The difference in magnitude of GO impact between water and sediment communities associated to Turbiscan analysis confirm that the GO is more bioavailable for microbial communities from the sediment rather than for free living microorganisms from the water column. The presence of a complex biofilm containing diatoms *N.palea* and bacteria also contribute to this change of bioavailability. Indeed, these microorganisms were shown to stabilize CBNs in the biofilm through secretion of extracellular polymeric substances (EPS) [70–72]. Thus, the trapping of GO may decrease its bioavailability for bacteria from the water column while it would increase the occurrence of direct contact with bacteria in the biofilm (*i.e.* and other benthic organisms). This direct contact was evidenced as the main mechanism of cytoxicity toward bacteria through impairment of cell membrane integrity [27,73,74].

Our data show that the biofilm compartment is more dynamic compared to free living bacteria as indicated by the time effect on diversity indexes from the control group. However, as there are no other organisms in the microcosms at T0, introduction of chironomids and newts between T0 and T1 would contribute mainly to the biofilm's dynamics through the increase in bacterial alpha diversity via the production of faeces, for example. In spite of this temporal dynamics inherent to microcosm experimental design as well as to this form of bacterial life [75], beta diversity measurement in pelagic as well as in benthic communities evidenced diverging phylogenetic trajectories in presence of GO compared to the control group. In this case, the stronger the contamination pressure is, the more communities are diverging. As the multiple species in biofilms may possess different sensitivity to GO, the decrease of affected taxa make available new ecological niches benefiting to less sensitive and more opportunistic species leading

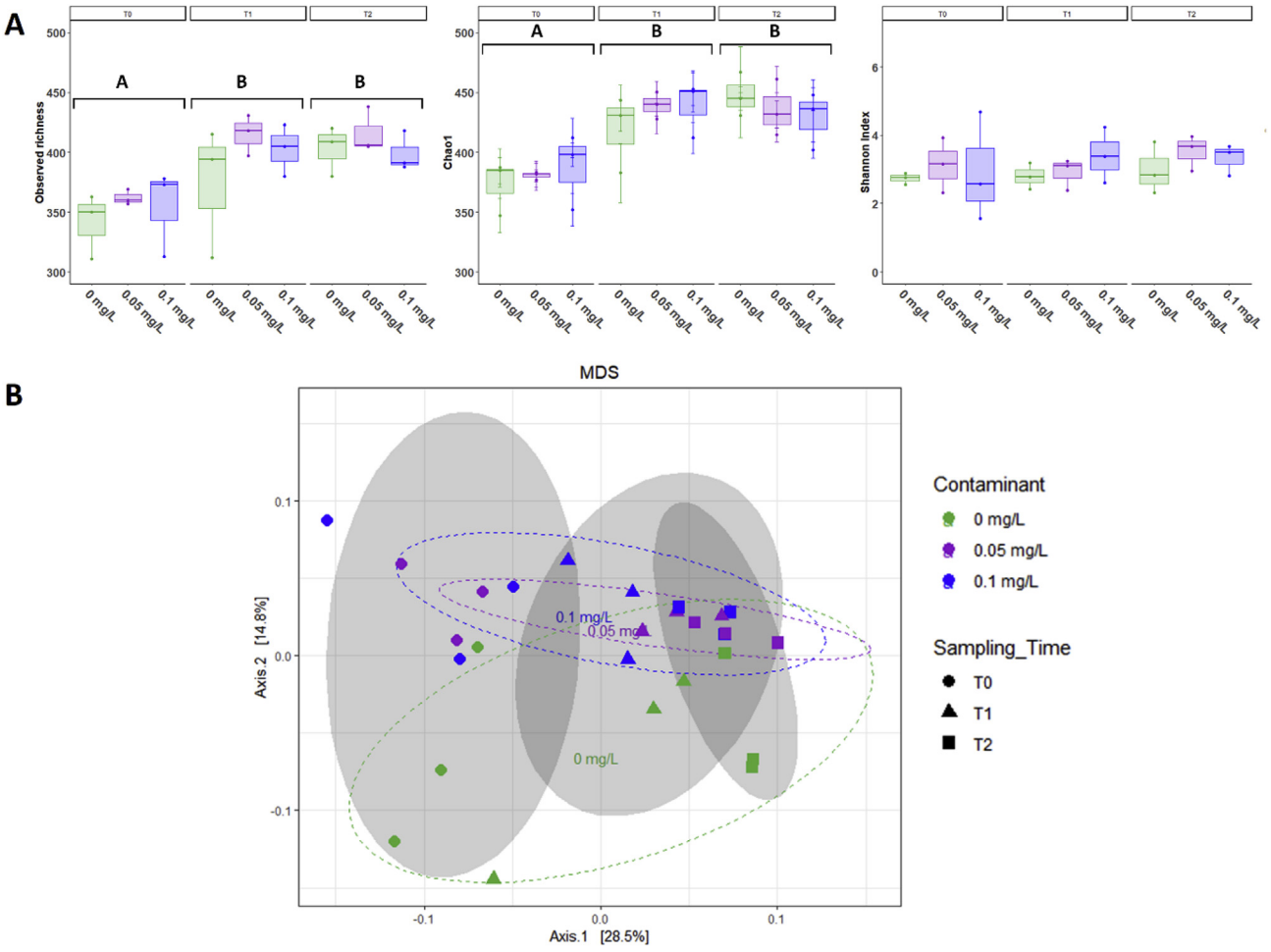

Fig. 4. Effects of exposure to GO on microbial communities in the sediment of the microcosms, as revealed by 16S amplicon sequencing. Observed richness, Chao1 and Shannon evenness indexes are compared between the three exposure conditions (0 mg L ^{1}, 0.05 mg L ^{1} and 0.1 mg L ^{1}) (A). MDS plot of bacterial communities based on unweighted Unifrac distances (B). Samples from different GO concentration are represented by different colors with 95% confidence ellipses, while different sampling times are represented by forms surrounded by 95% confidence ellipses in grey color. (A colour version of this figure can be viewed online.)

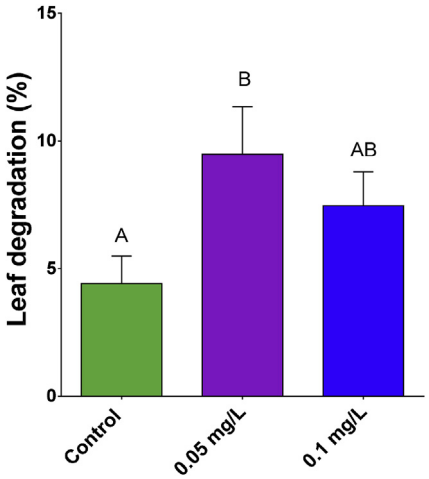

Fig. 5. Alder leaves degradation measured at the end of the exposure to 0, 0.05 or 0.1 mg L ^{1} of GO. Data are presented as mean ± SEM (n 39 leaves per condition). ANOVA $p < 0.05$ followed by Tukey test. Letters indicate significant differences between concentrations tested. (A colour version of this figure can be viewed online.)

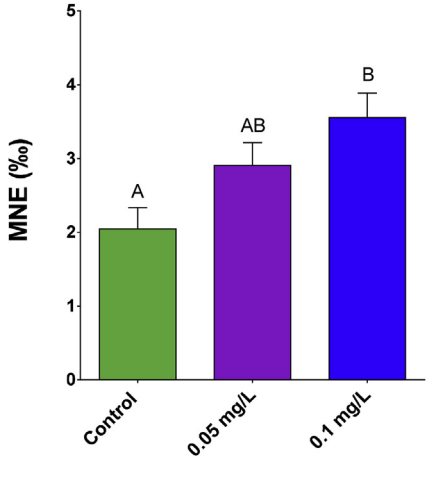

Fig. 6. Micronucleus induction measured in erythrocytes of *Pleurodeles waltl* exposed using microcosm to GO at T2 (10 days of exposure). Data are presented as mean ± SD (n 45 larvae per condition). Kruskal-Wallis $p < 0.01$ followed by multiple rank comparisons. Letters indicate significant differences between concentrations tested. (A colour version of this figure can be viewed online.)

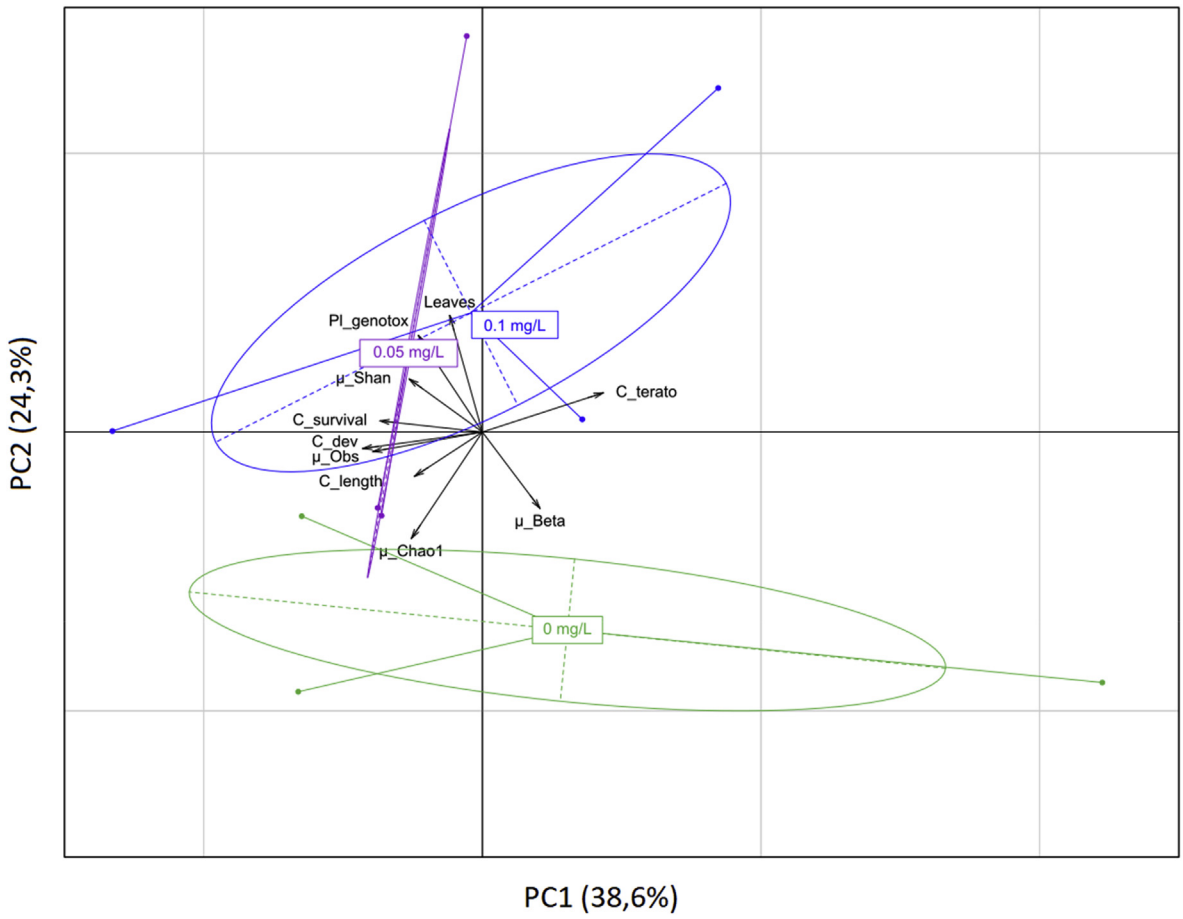

Fig. 7. Biplot of the first two components of principal component analysis (PCA) including biological responses measured in different conditions of GO exposure (0, 0.05 or 0.1 mg L ^{1}). Axis 1: 38.6%, Axis 2: 24,3%. Pl pleurodeles, C Chironomus, dev development stage, terato teratogenesis µ microorganisms, Obs Observed diversity, Shan Shannon index, Beta beta diversity, Leaves leaf litter degradation. (A colour version of this figure can be viewed online.)

to different equilibrium in microbial communities. Thus, the phyla Planctomycetes, Armatimonadetes and WPS 2 appear tolerant to GO as their relative abundances increased in the exposed condi tions. A similar trend was previously evidenced for Planctomycetes from soil bacterial communities exposed to GO [76] or silver nanoparticles [77]. These changes would contribute to the di vergences in the evolution of the biofilm composition between the tested conditions. However, as a dynamic system, it is possible that the direct toxicity of GO will be attenuated with biofilm maturation. Indeed, it was previously observed in bacterial biofilm using *E. coli* or *S. aureus* models that after 48 h of exposure, corresponding to the mature phase of biofilm, cell growth inhibition and induction of ROS production by rGO was suppressed, even at concentrations up to 100 mg L^{-1} [78]. This study also indicated that bacteria were able to oxidize rGO into GO. Transformations of the tested material potentially occurring under our experimental conditions are remaining to be assessed when technological barriers will be overcome.

4.3. Effects on chironomid larvae and consequences for leaf litter degradation

No apparent toxicity on growth and teratogenicity could be highlighted on chironomids. The low amount of larvae remaining at the end of the exposure could be only related to predation by Pleurodeles larvae that is more likely to occur within the last days of the experiment when they reach larger sizes [43,79]. It is also possible that the apparent no effects on chironomids may result from a preferential predation by pleurodeles larvae of affected chironomids. However, the low sensitivity of chironomids toward CBNs was previously indicated for fullerene [80], multi walled carbon nanotubes [81] as well as GO [67]. In the later study, no effects were observed on chironomids after 9 days of exposure to GO at concentrations up to 100 mg L^{-1}, which is consistent with the present results and corroborate the predation hypothesis without any pressure of selection.

Chironomids are shredders, deposit feeders that preferentially feed on biofilm rather than non living organic matter [82]. Despite the known implication of bacteria in this ecological process, chi ronomids constitute the main decomposers of organic matter in such time duration experiment [22]. Despite the pressure of pre dation on chironomids, the alder leaves decomposition process is maintained. In this study, it appears that this process increases in presence of GO while opposite results were observed in the case of contamination by other nanoparticles [22,83]. It was previously observed through the comparison of deformities in the mouthparts of chironomids sampled in differentially contaminated sites that teratogenicity was associated with lower leaves degradation ac tivities [84]. In the present study, no teratogenicity was measured and as PCA results indicated an independence of these variables, we can suggest that the increase of leaves consumption is associated to indirect effects. The presence of GO in the biofilm might influence their feeding behaviour through two possible ways. 1) Changes in bacterial communities and GO trapping might decrease the biofilm

palatability. Indeed, it was demonstrated that food quality prevails on contaminant concentration for chironomids food source selection [85]. Thus, the loss of biofilm palatability and quality would lead to preferential feeding on alder leaves. 2) The presence of GO at low concentration may increase fungus development as it was demonstrated that GBMs could stimulate the growth of rot fungus at "low concentration" without influencing the decomposition activity [86,87]. Thus, an increase in fungus biomass on leaves would improve their palatability and influence chironomids feeding behaviour [88,89]. According to the PCA results, it seems that there is a correlation between the diversity of microorganism species from the biofilm and the development of chironomids that is consistent with the first hypothesis. It is interesting to note that in any case, this change of behaviour had no measurable consequence on chironomids development. Modifications of the feeding behaviour could also theoretically contribute to changes observed in bacterial community compositions. Indeed, diet changes could lead to modification of chironomids gut microbiota and modify microbial composition of the faeces rejected into the mesocosms.

These changes in organic matter decomposition could potentially lead to changes in carbon and nutrient cycling, influencing energy flows of the system [90] but it remains to be determined whether or not it is occurring under these conditions. Thus, litter decomposition appears as an interesting marker integrating direct and indirect toxicological effects occurring at the lower trophic levels.

4.4. Effects on pleurodeles larvae

The results obtained in this experiment indicated that GO is able to induce genotoxic effects *in vivo* at low concentration under realistic environmental conditions. Genotoxic potential of GO was also observed in other organisms such as mice after repeated or single injection of GO at concentrations ranging from 0.01 to 20 mg kg^{-1} [91,92]. This was also observed in the amphibians *Xenopus laevis* [42], which is consistent with the present results. In the latter study case, tadpoles were exposed during 12 days to the same commercial GO as the one used in the current microcosm study. The genotoxic response measured in *X. laevis* after exposure to 0.1 mg L^{-1} was associated to oxidative stress and pro inflammatory response leading to an increase in circulating micronucleated erythrocytes [42]. Despite important biological differences between these two amphibian model species, it can be suggested that the genotoxic effects observed in Pleurodeles resulted from similar pathways. Under our experimental conditions, Pleurodeles larvae were exposed to GO through two pathways simultaneously: direct exposure due to the presence of GO in the media as well as dietary exposure by feeding on contaminated chironomids. However, PCA analysis indicated that the marker of genotoxicity was independent from those associated to other trophic levels, which reinforces the hypothesis of effects associated to direct exposure over trophic effects. In the case of a direct exposure, as the contamination was performed sequentially and according to previous study indicating that at least 4 days of exposure to a genotoxic compound are necessary to induce the formation of micronuclei [47], we can suggest that a concentration of 0.8 mg L^{-1} of GO is able to induce genotoxic effects (concentration reached 4 days before the sampling). It seems that the predation behaviour of the Pleurodeles was not influenced by GO exposure. This is supported by the high decrease in chironomid larvae as well as the absence of differences within the chironomids survival between the tested conditions at the end of the microcosm exposure. However, to date, it is not possible to evaluate separately the contribution of each pathway in the gen otoxic response observed.

5. Conclusion

This microcosm study allowed to identify the effects of a contamination by GO towards multiple interacting organisms and consequences on ecosystem functioning. Analysis indicated that GO could induce toxicological effects in top predators as well as in microorganisms at environmentally relevant concentration [93]. Genotoxicity was evidenced in top predators while bacterial communities were modified after GO exposure. Communities from the sediment were shown to be more impacted than those from the water column due to sedimentation of the GO under more realistic environmental conditions. Even if no toxicity was observed for chironomids, indirect effects were highlighted and led to changes in the decomposition of organic matter in the system.

This experiment allowed to better encompass ecotoxicity of GO under realistic conditions and supports the need to develop the use of more complex systems including trophic chains in ecotoxicity assessment. Indeed, the use of these experimental systems may evidence routes of exposure that are poorly or not estimated in classical standardized tests based on single species assessments.

Conflicts of interest

The authors declare no conflict of interest.

Acknowledgments

This project has received funding from the European Union's Horizon 2020 research and innovation programme under grant agreement No 696656 and No 78519. This research was also supported by the French Ministry of National Education, Higher Education and Research. We would like to thank Alpha Diallo for the support during the experiment.

Appendix A. Supplementary data

Supplementary data to this article can be found online at https://doi.org/10.1016/j.carbon.2019.09.051.

References

[1] A. Ali Tahir, H. Ullah, P. Sudhagar, M. Asri Mat Teridi, A. Devadoss, S. Sundaram, The application of graphene and its derivatives to energy conversion, storage, and environmental and biosensing devices, Chem. Rec. 16 (2016) 1591 1634, https://doi.org/10.1002/tcr.201500279.
[2] J. Liu, L. Cui, D. Losic, Graphene and graphene oxide as new nanocarriers for drug delivery applications, Acta Biomater. 9 (2013) 9243 9257, https://doi.org/10.1016/j.actbio.2013.08.016.
[3] B.H. Nguyen, V.H. Nguyen, Promising applications of graphene and graphene-based nanostructures, Adv. Nat. Sci. Nanosci. Nanotechnol. 7 (2016), 023002, https://doi.org/10.1088/2043-6262/7/2/023002.
[4] F. Perreault, A. Fonseca de Faria, M. Elimelech, Environmental applications of graphene-based nanomaterials, Chem. Soc. Rev. 44 (2015) 5861 5896, https://doi.org/10.1039/C5CS00021A.
[5] K. Scida, P.W. Stege, G. Haby, G.A. Messina, C.D. García, Recent applications of carbon-based nanomaterials in analytical chemistry: critical review, Anal. Chim. Acta 691 (2011) 6 17, https://doi.org/10.1016/j.aca.2011.02.025.
[6] O.C. Compton, S.T. Nguyen, Graphene oxide, highly reduced graphene oxide, and graphene: versatile building blocks for carbon-based materials, Small 6 (2010) 711 723.
[7] R. Arvidsson, S. Molander, B.A. Sandén, Review of potential environmental and health risks of the nanomaterial graphene, Hum. Ecol. Risk Assess. Int. J. 19 (2013) 873 887, https://doi.org/10.1080/10807039.2012.702039.
[8] B. Fadeel, C. Bussy, S. Merino, E. Vázquez, E. Flahaut, F. Mouchet, L. Evariste, L. Gauthier, A.J. Koivisto, U. Vogel, C. Martín, L.G. Delogu, T. Buerki-Thurnherr,

P. Wick, D. Beloin-Saint-Pierre, R. Hischier, M. Pelin, F. Candotto Carniel, M. Tretiach, F. Cesca, F. Benfenati, D. Scaini, L. Ballerini, K. Kostarelos, M. Prato, A. Bianco, Safety assessment of graphene-based materials: focus on human health and the environment, ACS Nano 12 (2018) 10582 10620, https://doi.org/10.1021/acsnano.8b04758.
[9] A.A. Keller, S. McFerran, A. Lazareva, S. Suh, Global life cycle releases of engineered nanomaterials, J. Nanoparticle Res. 15 (2013), https://doi.org/10.1007/s11051-013-1692-4.
[10] A. Mottier, F. Mouchet, É. Pinelli, L. Gauthier, E. Flahaut, Environmental impact of engineered carbon nanoparticles: from releases to effects on the aquatic biota, Curr. Opin. Biotechnol. 46 (2017) 1 6, https://doi.org/10.1016/j.copbio.2016.11.024.
[11] J. Zhao, Z. Wang, J.C. White, B. Xing, Graphene in the aquatic environment: adsorption, dispersion, toxicity and transformation, Environ. Sci. Technol. 48 (2014) 9995 10009, https://doi.org/10.1021/es5022679.
[12] L. Ou, B. Song, H. Liang, J. Liu, X. Feng, B. Deng, T. Sun, L. Shao, Toxicity of graphene-family nanoparticles: a general review of the origins and mechanisms, Part, Part. Fibre Toxicol. 13 (2016), https://doi.org/10.1186/s12989-016-0168-y.
[13] A.B. Seabra, A.J. Paula, R. de Lima, O.L. Alves, N. Durán, Nanotoxicity of graphene and graphene oxide, Chem. Res. Toxicol. 27 (2014) 159 168, https://doi.org/10.1021/tx400385x.
[14] Z. Singh, Toxicity of graphene and its nanocomposites to human cell lines-the present scenario, Int. J. Biomed. Clin. Sci. 1 (2016) 24 29.
[15] A.M. Jastrzębska, A.R. Olszyna, The ecotoxicity of graphene family materials: current status, knowledge gaps and future needs, J. Nanoparticle Res. 17 (2015) 40, https://doi.org/10.1007/s11051-014-2817-0.
[16] A. Montagner, S. Bosi, E. Tenori, M. Bidussi, A.A. Alshatwi, M. Tretiach, M. Prato, Z. Syrgiannis, Ecotoxicological effects of graphene-based materials, 2D Mater. 4 (2016), 012001, https://doi.org/10.1088/2053-1583/4/1/012001.
[17] A. Bour, F. Mouchet, J. Silvestre, L. Gauthier, E. Pinelli, Environmentally relevant approaches to assess nanoparticles ecotoxicity: a review, J. Hazard Mater. 283 (2015) 764 777, https://doi.org/10.1016/j.jhazmat.2014.10.021.
[18] M. Garaud, M. Auffan, S. Devin, V. Felten, C. Pagnout, S. Pain-Devin, O. Proux, F. Rodius, B. Sohm, L. Giamberini, Integrated assessment of ceria nanoparticle impacts on the freshwater bivalve *Dreissena polymorpha*, Nanotoxicology 10 (2016) 935 944, https://doi.org/10.3109/17435390.2016.1146363.
[19] U. Hommen, B. Knopf, H. Rüdel, C. Schafers, K. De Schamphelaere, C. Schlekat, E.R. Garman, A microcosm study to support aquatic risk assessment of nickel: community-level effects and comparison with bioavailability-normalized species sensitivity distributions: aquatic microcosm study with Ni, Environ. Toxicol. Chem. 35 (2016) 1172 1182, https://doi.org/10.1002/etc.3255.
[20] R. Müller, C. Shinn, A.-M. Waldvogel, J. Oehlmann, R. Ribeiro, M. Moreira-Santos, Long-term effects of the fungicide pyrimethanil on aquatic primary producers in macrophyte-dominated outdoor mesocosms in two European ecoregions, Sci. Total Environ. 665 (2019) 982 994, https://doi.org/10.1016/j.scitotenv.2019.02.050.
[21] M. Auffan, M. Tella, C. Santaella, L. Brousset, C. Paillès, M. Barakat, B. Espinasse, E. Artells, J. Issartel, A. Masion, J. Rose, M.R. Wiesner, W. Achouak, A. Thiéry, J.-Y. Bottero, An adaptable mesocosm platform for performing integrated assessments of nanomaterial risk in complex environmental systems, Sci. Rep. 4 (2015), https://doi.org/10.1038/srep05608.
[22] A. Bour, F. Mouchet, S. Cadarsi, J. Silvestre, E. Chauvet, J.-M. Bonzom, C. Pagnout, H. Clivot, L. Gauthier, E. Pinelli, Impact of CeO $_2$ nanoparticles on the functions of freshwater ecosystems: a microcosm study, Environ. Sci. Nano. 3 (2016) 830 838, https://doi.org/10.1039/C6EN00116E.
[23] P.A. Holden, J.L. Gardea-Torresdey, F. Klaessig, R.F. Turco, M. Mortimer, K. Hund-Rinke, E.A. Cohen Hubal, D. Avery, D. Barceló, R. Behra, Y. Cohen, L. Deydier-Stephan, P.L. Ferguson, T.F. Fernandes, B. Herr Harthorn, W.M. Henderson, R.A. Hoke, D. Hristozov, J.M. Johnston, A.B. Kane, L. Kapustka, A.A. Keller, H.S. Lenihan, W. Lovell, C.J. Murphy, R.M. Nisbet, E.J. Petersen, E.R. Salinas, M. Scheringer, M. Sharma, D.E. Speed, Y. Sultan, P. Westerhoff, J.C. White, M.R. Wiesner, E.M. Wong, B. Xing, M. Steele Horan, H.A. Godwin, A.E. Nel, Considerations of environmentally relevant test conditions for improved evaluation of ecological hazards of engineered nanomaterials, Environ. Sci. Technol. 50 (2016) 6124 6145, https://doi.org/10.1021/acs.est.6b00608.
[24] H. Ji, H. Sun, X. Qu, Antibacterial applications of graphene-based nanomaterials: recent achievements and challenges, Adv. Drug Deliv. Rev. 105 (2016) 176 189, https://doi.org/10.1016/j.addr.2016.04.009.
[25] A. Lukowiak, A. Kedziora, W. Strek, Antimicrobial graphene family materials: progress, advances, hopes and fears, Adv. Colloid Interface Sci. 236 (2016) 101 112, https://doi.org/10.1016/j.cis.2016.08.002.
[26] M. Yousefi, M. Dadashpour, M. Hejazi, M. Hasanzadeh, B. Behnam, M. de la Guardia, N. Shadjou, A. Mokhtarzadeh, Anti-bacterial activity of graphene oxide as a new weapon nanomaterial to combat multidrug-resistance bacteria, Mater. Sci. Eng. C 74 (2017) 568 581, https://doi.org/10.1016/j.msec.2016.12.125.
[27] S. Liu, T.H. Zeng, M. Hofmann, E. Burcombe, J. Wei, R. Jiang, J. Kong, Y. Chen, Antibacterial activity of graphite, graphite oxide, graphene oxide, and reduced graphene oxide: membrane and oxidative stress, ACS Nano 5 (2011) 6971 6980, https://doi.org/10.1021/nn202451x.
[28] X. Hu, K. Lu, L. Mu, J. Kang, Q. Zhou, Interactions between graphene oxide and plant cells: regulation of cell morphology, uptake, organelle damage, oxidative effects and metabolic disorders, Carbon 80 (2014) 665 676, https://doi.org/10.1016/j.carbon.2014.09.010.
[29] J. Zhao, X. Cao, Z. Wang, Y. Dai, B. Xing, Mechanistic understanding toward the toxicity of graphene-family materials to freshwater algae, Water Res. 111 (2017) 18 27, https://doi.org/10.1016/j.watres.2016.12.037.
[30] T. Mesaric, C. Gambardella, T. Milivojević, M. Faimali, D. Drobne, C. Falugi, D. Makovec, A. Jemec, K. Sepcić, High surface adsorption properties of carbon-based nanomaterials are responsible for mortality, swimming inhibition, and biochemical responses in Artemia salina larvae, Aquat. Toxicol. 163 (2015) 121 129, https://doi.org/10.1016/j.aquatox.2015.03.014.
[31] T. Mesarič, K. Sepčič, V. Piazza, C. Gambardella, F. Garaventa, D. Drobne, M. Faimali, Effects of nano carbon black and single-layer graphene oxide on settlement, survival and swimming behaviour of Amphibalanus amphitrite larvae, Chem. Ecol. 29 (2013) 643 652, https://doi.org/10.1080/02757540.2013.817563.
[32] L. Lagier, F. Mouchet, C. Laplanche, A. Mottier, S. Cadarsi, L. Evariste, C. Sarrieu, P. Lonchambon, E. Pinelli, E. Flahaut, L. Gauthier, Surface area of carbon-based nanoparticles prevails on dispersion for growth inhibition in amphibians, Carbon 119 (2017) 72 81, https://doi.org/10.1016/j.carbon.2017.04.016.
[33] F. Rimet, A. Bouchez, Life-forms, cell-sizes and ecological guilds of diatoms in European rivers, Knowl. Manag. Aquat. Ecosyst. (2012), https://doi.org/10.1051/kmae/2012018.
[34] P.H. Adler, G.W. Courtney, Ecological and societal services of aquatic Diptera, Insects 10 (2019) 70, https://doi.org/10.3390/insects10030070.
[35] B. Oertli, J. Biggs, R. Céréghino, P. Grillas, P. Joly, J.-B. Lachavanne, Conservation and monitoring of pond biodiversity: introduction, Aquat. Conserv. Mar. Freshw. Ecosyst. 15 (2005) 535 540, https://doi.org/10.1002/aqc.752.
[36] L.L. Barton, R.J.C. McLean, Environmental Microbiology and Microbial Ecology, John Wiley & Sons, 2019.
[37] L. Gauthier, F. Mouchet, Chapter 15 genotoxicity in urodele Amphibians Pleurodeles waltl and Ambystoma mexicanum (Lissamphibia, Caudata) exposed to freshwater pollutants: a historical view, in: Ecotoxicol. Genotoxicol. Non-tradit. Aquat. Models, The Royal Society of Chemistry, 2017, pp. 347 370, https://doi.org/10.1039/9781782629887-00347.
[38] J. Salmelin, K.M. Vuori, H. Hamalainen, Inconsistency in the analysis of morphological deformities in chironomidae (Insecta: Diptera) larvae, Environ. Toxicol. Chem. 34 (2015) 1891 1898, https://doi.org/10.1002/etc.3010.
[39] Susan Anderson, Walter Sadinski, Lee Shugart, Peter Brussard, Michael Depledge, Tim Ford, JoEllen Hose, John Stegeman, William Suk, Isaac Wirgin, Gerald Wogan, Genetic and molecular ecotoxicology: a research framework, Environ. Health Perspect. 102 (1994) 3 8, https://doi.org/10.1289/ehp.94102s123.
[40] C. Pascoal, F. Cássio, A. Marcotegui, B. Sanz, P. Gomes, Role of fungi, bacteria, and invertebrates in leaf litter breakdown in a polluted river, J. North Am. Benthol. Soc. 24 (2005) 784 797, https://doi.org/10.1899/05-010.1.
[41] B. Lobato, C. Merino, V. Barranco, T.A. Centeno, Large-scale conversion of helical-ribbon carbon nanofibers to a variety of graphene-related materials, RSC Adv. 6 (2016) 57514 57520, https://doi.org/10.1039/C6RA08865A.
[42] L. Evariste, L. Lagier, P. Gonzalez, A. Mottier, F. Mouchet, S. Cadarsi, P. Lonchambon, G. Daffe, G. Chimowa, C. Sarrieu, E. Ompraret, A.-M. Galibert, C.M. Ghimbeu, E. Pinelli, E. Flahaut, L. Gauthier, Thermal reduction of graphene oxide mitigates its in vivo genotoxicity toward Xenopus laevis tadpoles, Nanomaterials 9 (2019) 584, https://doi.org/10.3390/nano9040584.
[43] A. Bour, F. Mouchet, S. Cadarsi, J. Silvestre, L. Verneuil, D. Baqué, E. Chauvet, J.-M. Bonzom, C. Pagnout, H. Clivot, I. Fourquaux, M. Tella, M. Auffan, L. Gauthier, E. Pinelli, Toxicity of CeO $_2$ nanoparticles on a freshwater experimental trophic chain: a study in environmentally relevant conditions through the use of mesocosms, Nanotoxicology (2015) 1 11, https://doi.org/10.3109/17435390.2015.1053422.
[44] M. Tella, M. Auffan, L. Brousset, E. Morel, O. Proux, C. Chanéac, B. Angeletti, C. Pailles, E. Artells, C. Santaella, J. Rose, A. Thiéry, J.-Y. Bottero, Chronic dosing of a simulated pond ecosystem in indoor aquatic mesocosms: fate and transport of CeO 2 nanoparticles, Environ. Sci. Nano. 2 (2015) 653 663, https://doi.org/10.1039/C5EN00092K.
[45] T. Marie, A. Mélanie, B. Lenka, I. Julien, K. Isabelle, P. Christine, M. Elise, S. Catherine, A. Bernard, A. Ester, R. Jérôme, T. Alain, B. Jean-Yves, Transfer, transformation, and impacts of ceria nanomaterials in aquatic mesocosms simulating a pond ecosystem, Environ. Sci. Technol. 48 (2014) 9004 9013, https://doi.org/10.1021/es501641b.
[46] I. Gallien, M. Durocher, Table chronologique du deyeloppement chez Pleurodeles waltlii, vol. 91, 1957, p. 97.
[47] A. Jaylet, P. Deparis, V. Ferrier, S. Grinfeld, R. Siboulet, A new micronucleus test using peripheral blood erythrocytes of the newt Pleurodeles waltl to detect mutagens in fresh-water pollution, Mutat. Res. Environ. Mutagen. Relat. Subj. 164 (1986) 245 257, https://doi.org/10.1016/0165-1161(86)90058-0.
[48] P.D. Nieuwkoop, J. Faber, Normal table of Xenopus laevis (Daudin). A systematical and chronological survey of the development from the fertilized egg till the end of metamorphosis, Q. Rev. Biol. 33 (1958), https://doi.org/10.1086/402265, 85 85.
[49] Y. Wang, P.-Y. Qian, Conservative fragments in bacterial 16S rRNA genes and primer design for 16S Ribosomal DNA amplicons in metagenomic studies, PLoS One 4 (2009), e7401, https://doi.org/10.1371/journal.pone.0007401.
[50] F. Escudié, L. Auer, M. Bernard, M. Mariadassou, L. Cauquil, K. Vidal, S. Maman, G. Hernandez-Raquet, S. Combes, G. Pascal, FROGS: find, rapidly, OTUs with Galaxy solution, Bioinformatics 34 (2018) 1287 1294, https://doi.org/10.1093/bioinformatics/btx791.

[51] F. Mahé, T. Rognes, C. Quince, C. de Vargas, M. Dunthorn, Swarm: robust and fast clustering method for amplicon-based studies, PeerJ 2 (2014) e593, https://doi.org/10.7717/peerj.593.

[52] N.A. Bokulich, S. Subramanian, J.J. Faith, D. Gevers, J.I. Gordon, R. Knight, D.A. Mills, J.G. Caporaso, Quality-filtering vastly improves diversity estimates from Illumina amplicon sequencing, Nat. Methods 10 (2013) 57 59, https://doi.org/10.1038/nmeth.2276.

[53] C. Quast, E. Pruesse, P. Yilmaz, J. Gerken, T. Schweer, P. Yarza, J. Peplies, F.O. Glockner, The SILVA ribosomal RNA gene database project: improved data processing and web-based tools, Nucleic Acids Res. 41 (2012) D590 D596, https://doi.org/10.1093/nar/gks1219.

[54] P.J. McMurdie, S. Holmes, phyloseq: an R package for reproducible interactive analysis and graphics of microbiome census data, PLoS One 8 (2013), e61217, https://doi.org/10.1371/journal.pone.0061217.

[55] M.I. Love, W. Huber, S. Anders, Moderated estimation of fold change and dispersion for RNA-seq data with DESeq2, Genome Biol. 15 (2014), https://doi.org/10.1186/s13059-014-0550-8.

[56] J. Oksanen, F.G. Blanchet, R. Kindt, P. Legendre, P.R. Minchin, R.B. O'hara, G.L. Simpson, P. Solymos, M.H.H. Stevens, H. Wagner, Package 'vegan,' Community Ecol. Package Version. 2, 2015.

[57] S. Dray, A.-B. Dufour, The ade4 package: implementing the duality diagram for ecologists, J. Stat. Softw. 22 (2007) 1 20, https://doi.org/10.18637/jss.v022.i04.

[58] D.G. Goodwin, A.S. Adeleye, L. Sung, K.T. Ho, R.M. Burgess, E.J. Petersen, Detection and quantification of Graphene-family nanomaterials in the environment, Environ. Sci. Technol. 52 (2018) 4491 4513, https://doi.org/10.1021/acs.est.7b04938.

[59] A. Al-Jumaili, S. Alancherry, K. Bazaka, M. Jacob, Review on the antimicrobial properties of carbon nanostructures, Materials 10 (2017) 1066, https://doi.org/10.3390/ma10091066.

[60] H.E. Karahan, C. Wiraja, C. Xu, J. Wei, Y. Wang, L. Wang, F. Liu, Y. Chen, Graphene materials in antimicrobial nanomedicine: current status and future perspectives, Adv. Healthc. Mater. 7 (2018) 1701406, https://doi.org/10.1002/adhm.201701406.

[61] J. Zhu, J. Wang, J. Hou, Y. Zhang, J. Liu, B. Van der Bruggen, Graphene-based antimicrobial polymeric membranes: a review, J. Mater. Chem. A. 5 (2017) 6776 6793, https://doi.org/10.1039/C7TA00009J.

[62] J. Du, X. Hu, Q. Zhou, Graphene oxide regulates the bacterial community and exhibits property changes in soil, RSC Adv. 5 (2015) 27009 27017, https://doi.org/10.1039/C5RA01045D.

[63] T. Xiong, X. Yuan, H. Wang, L. Leng, H. Li, Z. Wu, L. Jiang, R. Xu, G. Zeng, Implication of graphene oxide in Cd-contaminated soil: a case study of bacterial communities, J. Environ. Manag. 205 (2018) 99 106, https://doi.org/10.1016/j.jenvman.2017.09.067.

[64] F. Ahmed, D.F. Rodrigues, Investigation of acute effects of graphene oxide on wastewater microbial community: a case study, J. Hazard Mater. 256 257 (2013) 33 39, https://doi.org/10.1016/j.jhazmat.2013.03.064.

[65] C. Guo, Y. Wang, Y. Luo, X. Chen, Y. Lin, X. Liu, Effect of graphene oxide on the bioactivities of nitrifying and denitrifying bacteria in aerobic granular sludge, Ecotoxicol. Environ. Saf. 156 (2018) 287 293, https://doi.org/10.1016/j.ecoenv.2018.03.036.

[66] X. Ren, J. Li, C. Chen, Y. Gao, D. Chen, M. Su, A. Alsaedi, T. Hayat, Graphene analogues in aquatic environments and porous media: dispersion, aggregation, deposition and transformation, Environ. Sci. Nano. 5 (2018) 1298 1340, https://doi.org/10.1039/C7EN01258F.

[67] V.L. Castro, Z. Clemente, C. Jonsson, M. Silva, J.H. Vallim, A.M.Z. de Medeiros, D.S.T. Martinez, Nanoecotoxicity assessment of graphene oxide and its relationship with humic acid: nanoecotoxicity of graphene oxide and humic acid, Environ. Toxicol. Chem. 37 (2018) 1998 2012, https://doi.org/10.1002/etc.4145.

[68] I. Chowdhury, M.C. Duch, N.D. Mansukhani, M.C. Hersam, D. Bouchard, Colloidal properties and stability of graphene oxide nanomaterials in the aquatic environment, Environ. Sci. Technol. 47 (2013) 6288 6296, https://doi.org/10.1021/es400483k.

[69] I. Chowdhury, N.D. Mansukhani, L.M. Guiney, M.C. Hersam, D. Bouchard, Aggregation and stability of reduced graphene oxide: complex roles of divalent cations, pH, and natural organic matter, Environ. Sci. Technol. 49 (2015) 10886 10893, https://doi.org/10.1021/acs.est.5b01866.

[70] M. Garacci, M. Barret, F. Mouchet, C. Sarrieu, P. Lonchambon, E. Flahaut, L. Gauthier, J. Silvestre, E. Pinelli, Few Layer Graphene sticking by biofilm of freshwater diatom Nitzschia palea as a mitigation to its ecotoxicity, Carbon 113 (2017) 139 150, https://doi.org/10.1016/j.carbon.2016.11.033.

[71] O.N. Ruiz, K.A.S. Fernando, B. Wang, N.A. Brown, P.G. Luo, N.D. McNamara, M. Vangsness, Y.-P. Sun, C.E. Bunker, Graphene Oxide: a nonspecific enhancer of cellular growth, ACS Nano 5 (2011) 8100 8107, https://doi.org/10.1021/nn202699t.

[72] L. Verneuil, J. Silvestre, I. Randrianjatovo, C.-E. Marcato-Romain, E. Girbal-Neuhauser, F. Mouchet, E. Flahaut, L. Gauthier, E. Pinelli, Double walled carbon nanotubes promote the overproduction of extracellular protein-like polymers in Nitzschia palea: an adhesive response for an adaptive issue, Carbon 88 (2015) 113 125, https://doi.org/10.1016/j.carbon.2015.02.053.

[73] R.G. Combarros, S. Collado, M. Díaz, Toxicity of graphene oxide on growth and metabolism of Pseudomonas putida, J. Hazard Mater. 310 (2016) 246 252, https://doi.org/10.1016/j.jhazmat.2016.02.038.

[74] S.M. Dizaj, A. Mennati, S. Jafari, K. Khezri, K. Adibkia, Antimicrobial activity of carbon-based nanoparticles, Adv. Pharmaceut. Bull. 5 (2015) 19.

[75] I.W. Sutherland, The biofilm matrix an immobilized but dynamic microbial environment, Trends Microbiol. 9 (2001) 222 227, https://doi.org/10.1016/S0966-842X(01)02012-1.

[76] C. Forstner, T.G. Orton, A. Skarshewski, P. Wang, P.M. Kopittke, P.G. Dennis, Effects of Graphene Oxide and Graphite on Soil Bacterial and Fungal Diversity, BioRxiv, 2019, p. 530485, https://doi.org/10.1101/530485.

[77] J. Wang, K. Shu, L. Zhang, Y. Si, Effects of silver nanoparticles on soil microbial communities and bacterial nitrification in suburban vegetable soils, Pedosphere 27 (2017) 482 490, https://doi.org/10.1016/S1002-0160(17)60344-8.

[78] Z. Guo, C. Xie, P. Zhang, J. Zhang, G. Wang, X. He, Y. Ma, B. Zhao, Z. Zhang, Toxicity and transformation of graphene oxide and reduced graphene oxide in bacteria biofilm, Sci. Total Environ. 580 (2017) 1300 1308, https://doi.org/10.1016/j.scitotenv.2016.12.093.

[79] M.I. Sánchez, A.J. Green, R. Alejandre, Shorebird predation affects density, biomass, and size distribution of benthic chironomids in salt pans: an exclosure experiment, J. North Am. Benthol. Soc. 25 (2006) 9 18.

[80] G.C. Waissi-Leinonen, E.J. Petersen, K. Pakarinen, J. Akkanen, M.T. Leppanen, J.V.K. Kukkonen, Toxicity of fullerene (C60) to sediment-dwelling invertebrate Chironomus riparius larvae, Environ. Toxicol. Chem. 31 (2012) 2108 2116, https://doi.org/10.1002/etc.1926.

[81] P. Martínez-Paz, V. Negri, A. Esteban-Arranz, J.L. Martínez-Guitarte, P. Ballesteros, M. Morales, Effects at molecular level of multi-walled carbon nanotubes (MWCNT) in Chironomus riparius (DIPTERA) aquatic larvae, Aquat. Toxicol. 209 (2019) 42 48, https://doi.org/10.1016/j.aquatox.2019.01.017.

[82] A. Widenfalk, A. Lundqvist, W. Goedkoop, Sediment microbes and biofilms increase the bioavailability of chlorpyrifos in Chironomus riparius (Chironomidae, Diptera), Ecotoxicol. Environ. Saf. 71 (2008) 490 497, https://doi.org/10.1016/j.ecoenv.2007.10.028.

[83] A. Pradhan, S. Seena, C. Pascoal, F. Cássio, Can metal nanoparticles be a threat to microbial decomposers of plant litter in streams? Microb. Ecol. 62 (2011) 58 68, https://doi.org/10.1007/s00248-011-9861-4.

[84] E.E. MacDonald, B.R. Taylor, Incidence of mentum deformities in midge larvae (Diptera:chironomidae) from Northern Nova Scotia, Canada, Hydrobiologia 563 (2006) 277 287, https://doi.org/10.1007/s10750-006-0012-8.

[85] E.M. De Haas, C. Wagner, A.A. Koelmans, M.H.S. Kraak, W. Admiraal, Habitat selection by chironomid larvae: fast growth requires fast food, J. Anim. Ecol. 75 (2006) 148 155, https://doi.org/10.1111/j.1365-2656.2005.01030.x.

[86] J. Xie, Z. Ming, H. Li, H. Yang, B. Yu, R. Wu, X. Liu, Y. Bai, S.-T. Yang, Toxicity of graphene oxide to white rot fungus Phanerochaete chrysosporium, Chemosphere 151 (2016) 324 331, https://doi.org/10.1016/j.chemosphere.2016.02.097.

[87] H. Yang, S. Feng, Q. Ma, Z. Ming, Y. Bai, L. Chen, S.-T. Yang, Influence of reduced graphene oxide on the growth, structure and decomposition activity of white-rot fungus *Phanerochaete chrysosporium*, RSC Adv. 8 (2018) 5026 5033, https://doi.org/10.1039/C7RA12364G.

[88] J.J. Casas, The effect of diet quality on growth and development of recently hatched larvae of Chironomus gr. plumosus, Limnética 12 (1996) 1 8.

[89] M.O. Gessner, E. Chauvet, M. Dobson, A perspective on leaf litter breakdown in streams, Oikos 85 (1999) 377 384, https://doi.org/10.2307/3546505.

[90] F.R. Hauer, G.A. Lamberti (Eds.), Methods in Stream Ecology, vol. 2, Acad. Press, Amsterdam, 2007.

[91] Y. Liu, Y. Luo, J. Wu, Y. Wang, X. Yang, R. Yang, B. Wang, J. Yang, N. Zhang, Graphene oxide can induce in vitro and in vivo mutagenesis, Sci. Rep. 3 (2013), https://doi.org/10.1038/srep03469.

[92] N.A. El-Yamany, F.F. Mohamed, T.A. Salaheldin, A.A. Tohamy, W.N. Abd El-Mohsen, A.S. Amin, Graphene oxide nanosheets induced genotoxicity and pulmonary injury in mice, Exp. Toxicol. Pathol. 69 (2017) 383 392, https://doi.org/10.1016/j.etp.2017.03.002.

[93] X. Zhang, Q. Zhou, W. Zou, X. Hu, Molecular mechanisms of developmental toxicity induced by Graphene Oxide at predicted environmental concentrations, Environ. Sci. Technol. 51 (2017) 7861 7871, https://doi.org/10.1021/acs.est.7b01922.

Assessment of graphene oxide ecotoxicity at several trophic levels using aquatic microcosms

Supplementary data

Lauris Evariste[1], Antoine Mottier[1], Laura Lagier[1], Stéphanie Cadarsi[1], Maialen Barret[1], Florence Mouchet[1*], Emmanuel Flahaut[2], Eric Pinelli[1] and Laury Gauthier[1]

[1]EcoLab, Université de Toulouse, CNRS, INPT, UPS, Toulouse, France

[2]CIRIMAT, Université de Toulouse, CNRS, INPT, UPS, UMR CNRS-UPS-INP N°5085, Université Toulouse 3 Paul Sabatier, Bât. CIRIMAT, 118 route de Narbonne, 31062 Toulouse cedex 9, France

*Corresponding author: florence.mouchet@ensat.fr

Tel: +33534323936

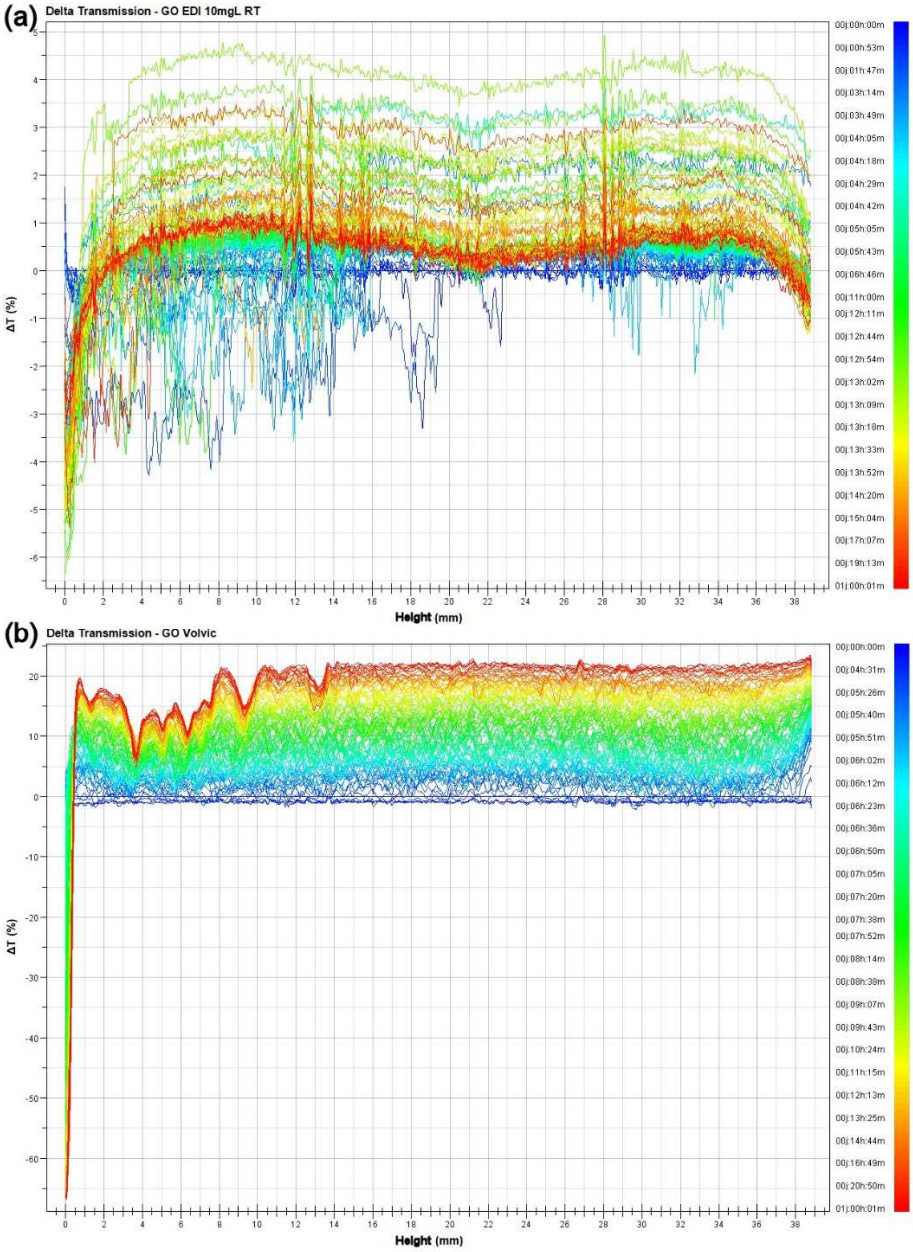

Figure S1: variation of the transmission *vs* time and height of the sample (compared to t0) of the suspensions of GO at 10 mg.L^{-1} in deionised water (EDI) (a) or Volvic water (b). Note the magnitude difference of the ΔT (%) scales.

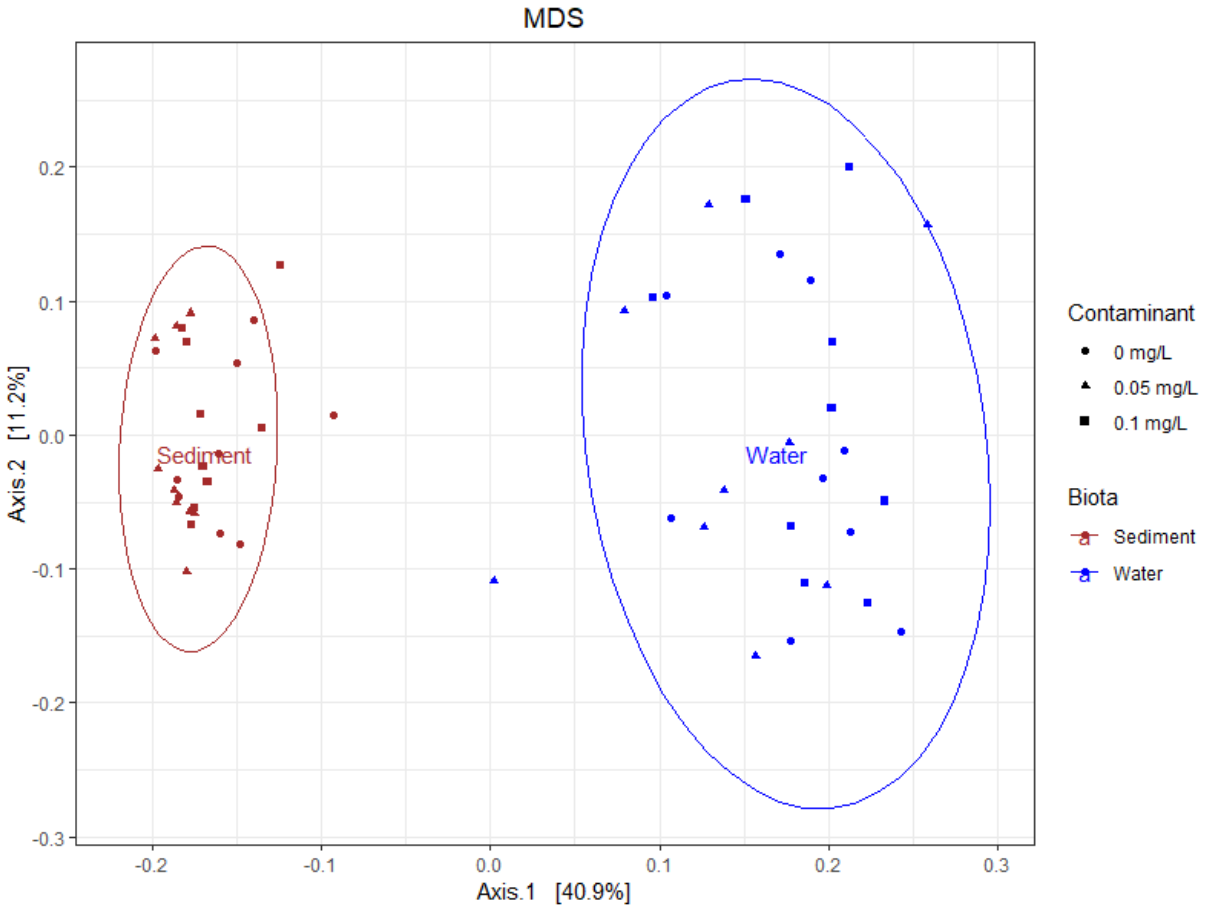

Figure S2: Multi-dimensional scaling analysis of microbiome data from the water (blue) and sediment (red) compartments. Ellipses were drawn with 95% confidence.

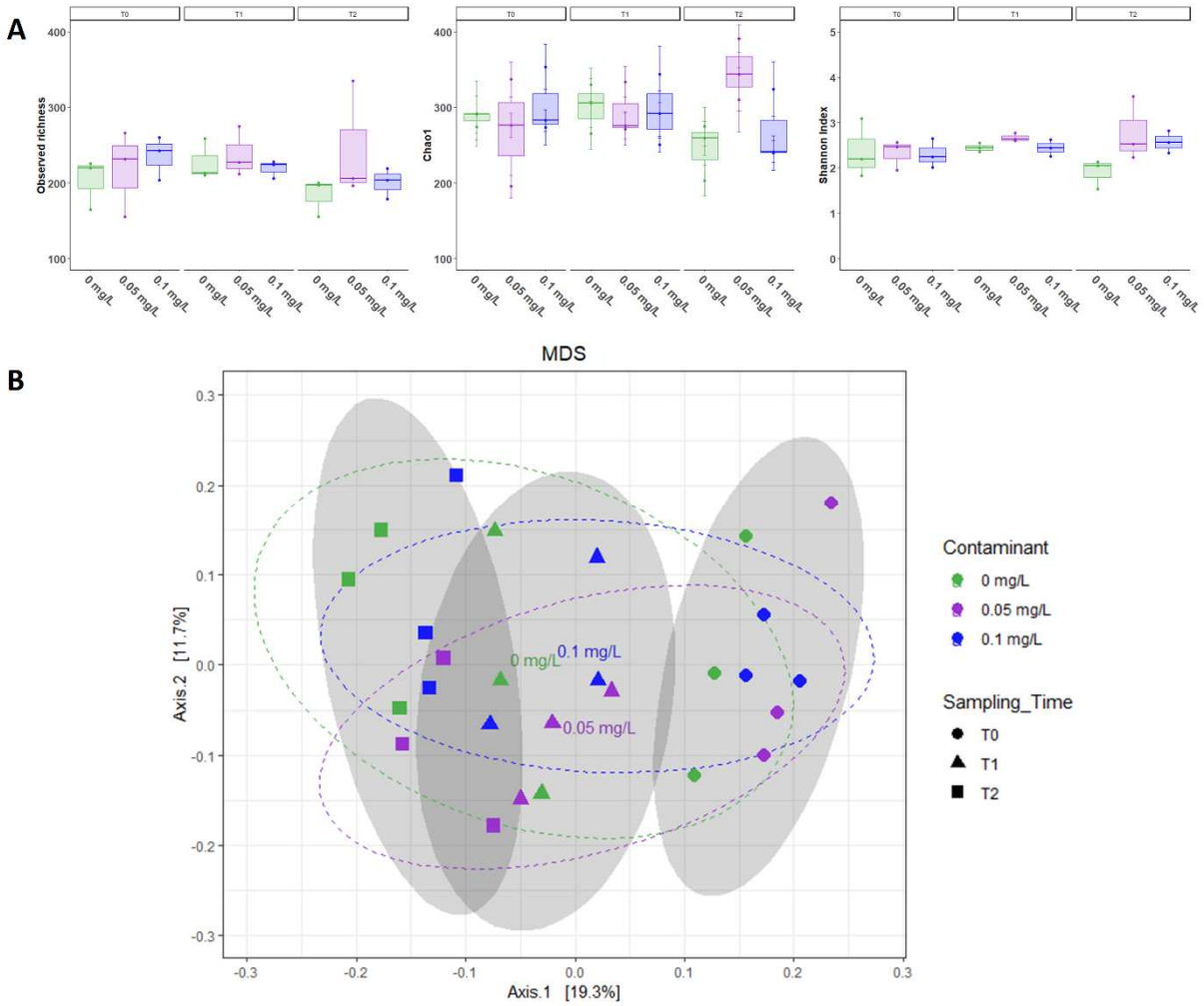

Figure S3: Effects of exposure to GO on bacterial communities from the water column of the microcosms as revealed by 16S amplicon sequencing. Observed richness, Chao1 and Shannon evenness indexes are compared between the three exposure conditions (0 $mg.L^{-1}$, 0.05 $mg.L^{-1}$ and 0.1 $mg.L^{-1}$). Observed richness, predicted richness and Shannon evenness index are compared between the three exposure conditions (0 mg/L, 0.05 mg/L and 0.1 mg/L) (A). MDS plot of bacterial communities based on unweighted Unifrac distances (B). Samples from different GO concentrations are represented by different colours with 95% confidence ellipses, while different sampling times are represented by forms surrounded by 95% confidence ellipses in grey.

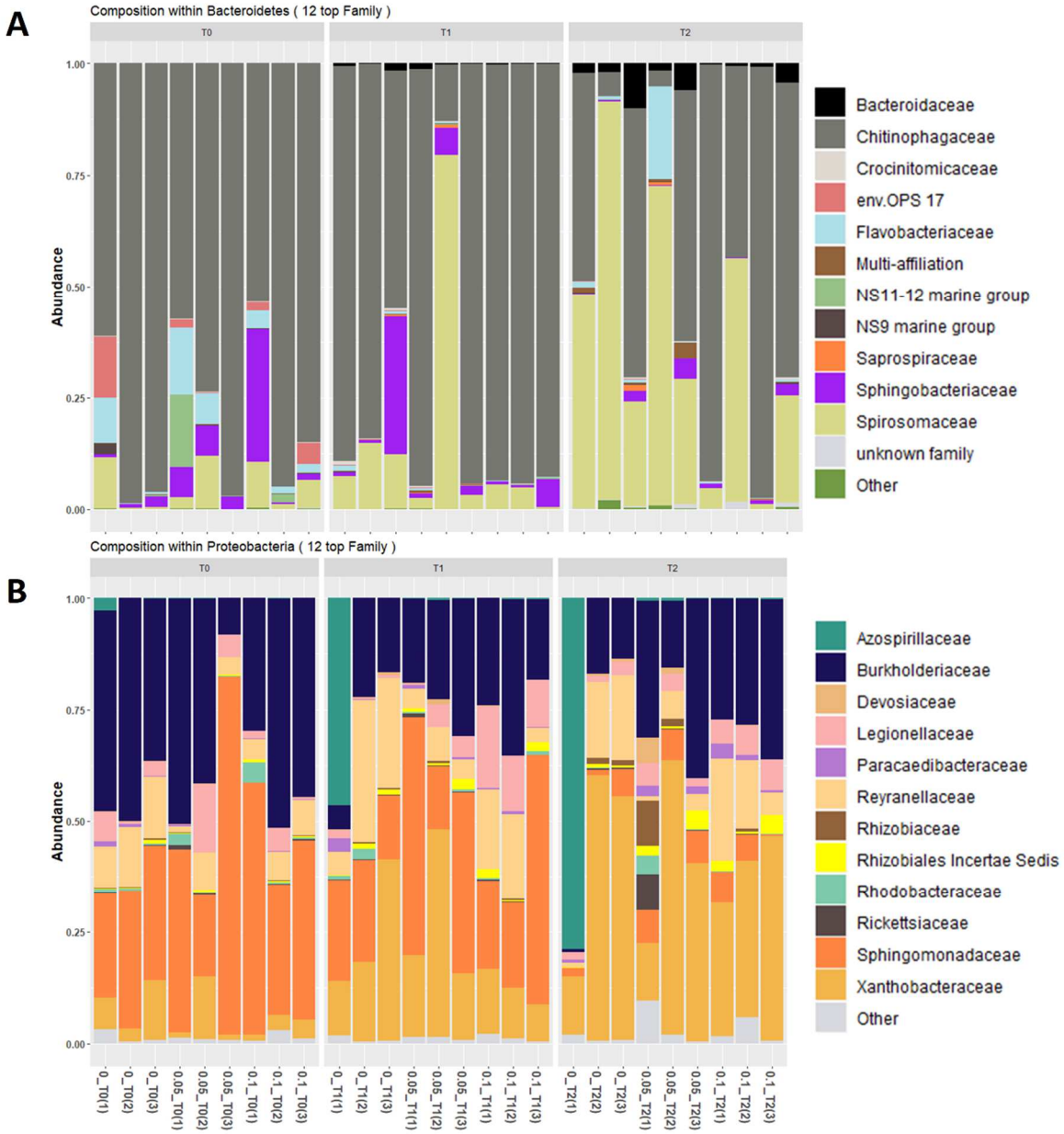

Figure S4: Relative abundance of bacterial families from phyla Bacteroidetes and Proteobacteria from the water column.

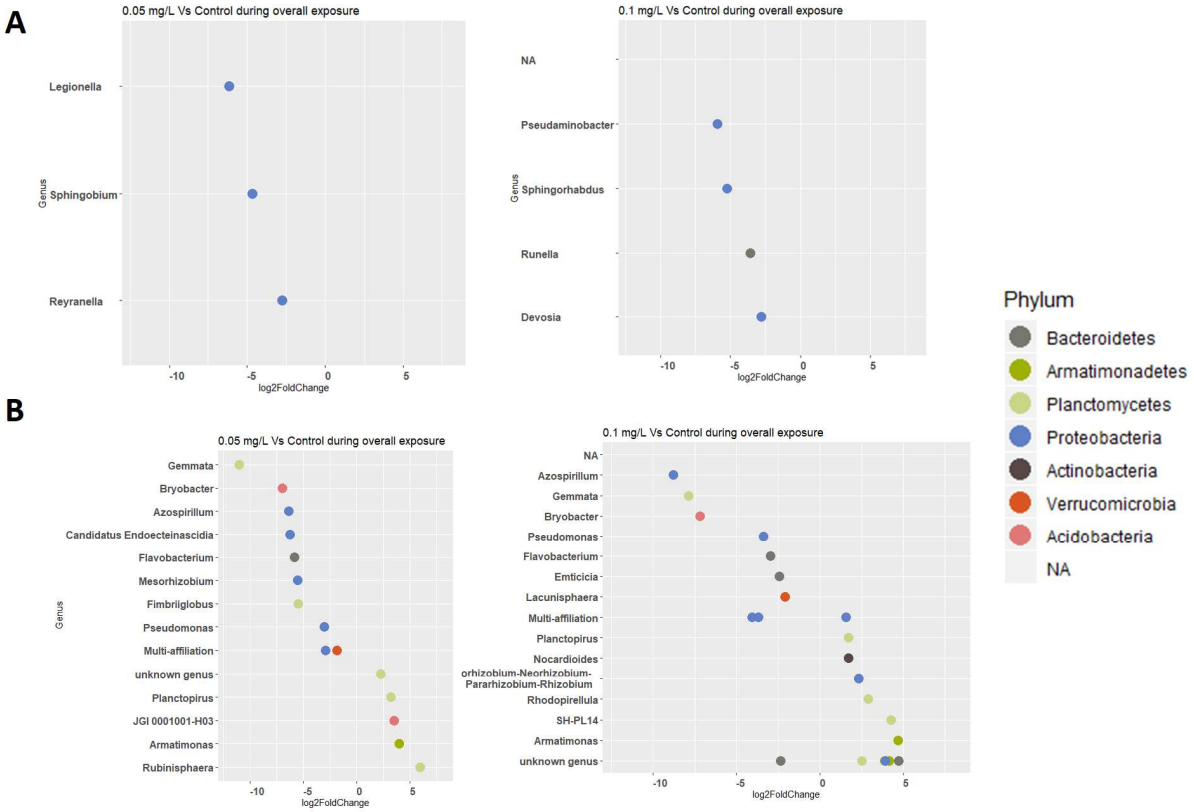

Figure S5: Bacterial genera differentially observed between the exposure conditions compared to the control during the whole experiment in the water compartment (A) and in the biofilm (B).

The relative abundance of genera *Gemmata*, *Azospirillum* and *Flavobacterium* were shown to decrease in a similar manner in the two GO conditions compared to the control group while genera *Planctopirus* and *Armatimonas* increased in the same order of manitude.

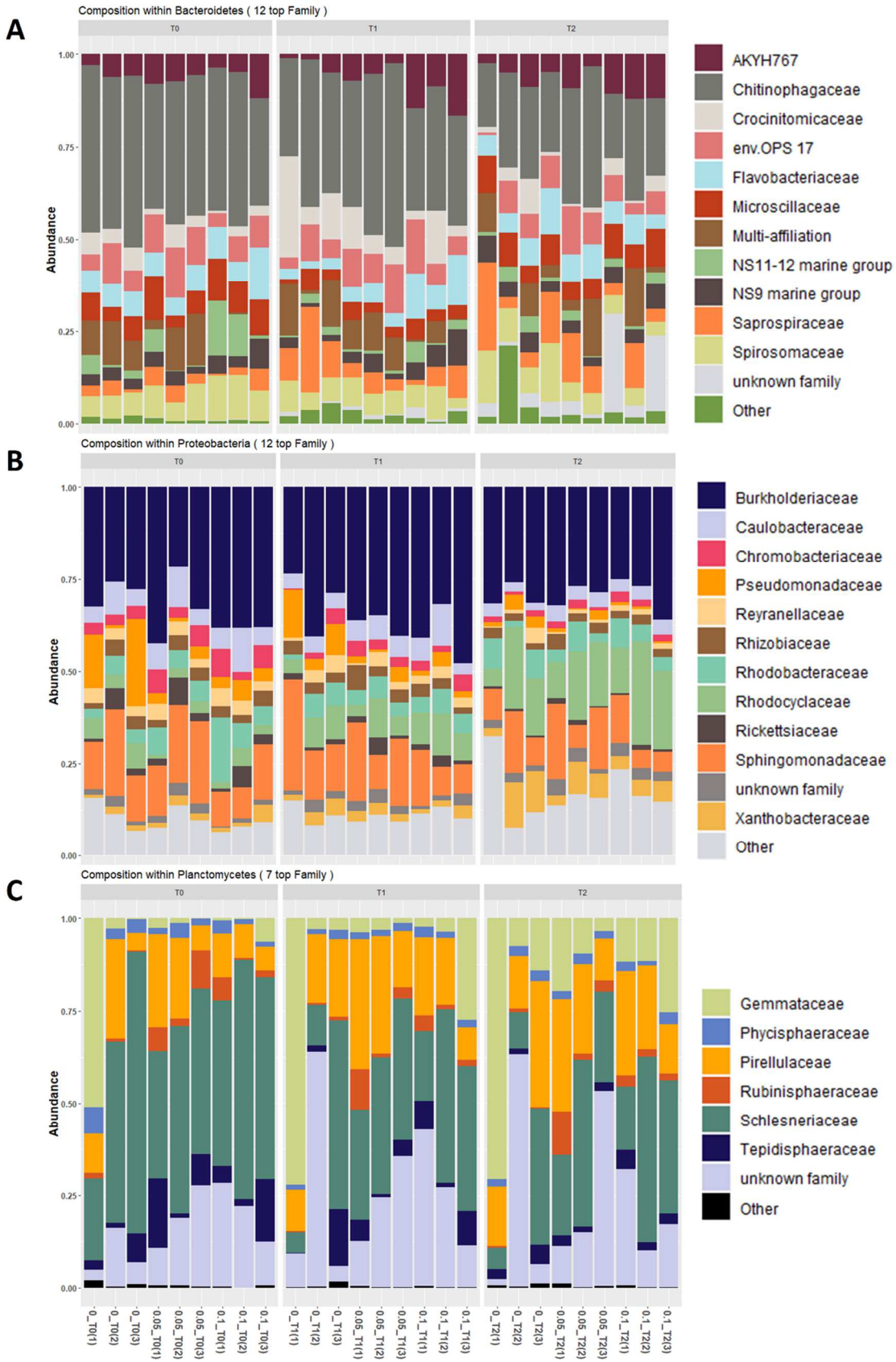

Figure S6: Relative abundance of bacterial families from phyla Bacteroidetes, Proteobacteria and Planctomycetes in the biofilm.

For families from the phylum Bacteroidetes, the relative abundance AKYH767 and NS9 significantly increased under the exposure condition of 0.1 mg/L of GO (Table S2). Relative abundance of family *Pseudomonadaceae* from phylum Proteobacteria significantly decreased at both concentrations of GO (Table S2) while for the phylum Planctomycetes, bacteria from family *Phycisphaeraceae*, *Rubinisphaeraceae* and *Schlesneriaceae* increased in presence of GO (Table S2).

Table S1: Dissolved Organic Carbon (DOC) measured in water of microcosms at three sampling times during the experiment.

	Condition		
Sampling	**0 $mg_{GO}.L^{-1}$**	**0.05 $mg_{GO}.L^{-1}$**	**0.1 $mg_{GO}.L^{-1}$**
T0	6.2 ± 3.6 $mg_{DOC}.L^{-1}$	5.1 ± 4.4 $mg_{DOC}.L^{-1}$	6 ± 5.2 $mg_{DOC}.L^{-1}$
T1	1.7 ± 0.2 $mg_{DOC}.L^{-1}$	1.9 ± 0.05 $mg_{DOC}.L^{-1}$	1.6 ± 0.6 $mg_{DOC}.L^{-1}$
T2	2.2 ± 0.06 $mg_{DOC}.L^{-1}$	2.4 ± 0.3 $mg_{DOC}.L^{-1}$	1.9 ± 0.2 $mg_{DOC}.L^{-1}$

Table S2: Table of results obtained from 2-ways ANOVA performed on data from the water column.

	Contaminant			Time of exposure			Contaminant*Time of exposure		
	Df	F-value	p-value	Df	F-value	p-value	Df	F-value	p-value
Phylum									
Acidobacteria	2	0.800	0.464	2	1.584	0.232	4	0.868	0.501
Actinobacteria	2	0.357	0.704	2	14.356	<0.001***	4	0.647	0.635
Armatimonadetes	2	2.423	0.117	2	0.120	0.887	4	0.704	0.599
Bacteroidetes	2	0.365	0.699	2	2.988	0.075	4	1.745	0.184
Chloroflexi	2	1.245	0.311	2	2.530	0.107	4	0.877	0.496
Ochrophyta	2	0.694	0.512	2	1.730	0.205	4	0.549	0.701
Cyanobacteria	2	0.859	0.440	2	0.544	0.589	4	1.040	0.413
Dependentiae	2	1.368	0.279	2	0.898	0.424	4	0.905	0.481
Firmicutes	2	1.731	0.205	2	4.539	0.025*	4	1.040	0.414
Fusobacteria	2	0.383	0.687	2	12.645	<0.001***	4	1.061	0.404
Planctomycetes	2	0.870	0.435	2	0.190	0.828	4	0.368	0.828
Proteobacteria	2	0.193	0.826	2	2.819	0.086	4	2.337	0.094
Spirochaetes	2	1.680	0.214	2	1.535	0.242	4	1.162	0.360
Verrucomicrobia	2	1.712	0.208	2	2.105	0.150	4	0.499	0.737
WPS-2	2	1.5	0.249	2	1.5	0.249	4	1.5	0.244
Family within Bacteroidetes									
Bacteroidaceae	2	0.511	0.608	2	10.927	<0.001***	4	0.184	0.943
Chitinophagaceae	2	0.583	0.568	2	3.897	0.039*	4	1.373	0.282
Crocinitomicaceae	2	2.322	0.126	2	3.082	0.070	4	1.780	0.176
env.OPS17	2	0.555	0.583	2	1.998	0.164	4	0.567	0.689
Flavobacteriaceae	2	1.526	0.244	2	1.123	0.346	4	0.475	0.753
NS11	2	0.786	0.470	2	1.473	0.255	4	0.796	0.543
NS9	2	0.926	0.400	2	1.096	0.355	4	0.798	0.541
Saprospiraceae	2	0.814	0.458	2	1.326	0.290	4	0.416	0.795
Sphingobacteriaceae	2	0.097	0.908	2	2.959	0.077	4	0.585	0.677
Spirosomaceae	2	0.089	0.915	2	2.467	0.113	4	0.132	0.968
Family within Proteobacteria									
Azospirillaceae	2	1.677	0.215	2	0.667	0.525	4	0.630	0.647
Burkholderiaceae	2	2.265	0.132	2	3.003	0.074	4	0.378	0.821
Devosiaceae	2	2.308	0.128	2	2.258	0.133	4	1.141	0.368
Legionellaceae	2	2.612	0.100	2	0.127	0.881	4	2.027	0.133
Paracaedibacteraceae	2	0.127	0.881	2	2.449	0.114	4	1.425	0.266
Reyranellaceae	2	3.956	0.037*	2	1.703	0.210	4	0.820	0.528
Rhizobiaceae	2	1.517	0.246	2	3.577	0.049*	4	1.364	0.285
Rhizobiales	2	1.214	0.320	2	3.266	0.061	4	0.610	0.660
Rhodobacteraceae	2	0.252	0.779	2	0.589	0.565	4	1.073	0.398
Rickettsiaceae	2	1.564	0.236	2	0.793	0.467	4	0.671	0.620
Sphingomonadaceae	2	2.286	0.102	2	11.325	<0.001***	4	1.324	0.298
Xanthobacteraceae	2	0.761	0.481	2	8.263	0.0028**	4	0.249	0.910

Table S3: Table of results obtained from 2-ways ANOVA performed on metagenomics data from the biofilm

	Contaminant			Time of exposure			Contaminant*Time of exposure		
	Df	F-value	p-value	Df	F-value	p-value	Df	F-value	p-value
Phylum									
Acidobacteria	2	5.119	0.0173*	2	1.641	0.221	4	3.119	0.041*
Actinobacteria	2	0.388	0.683	2	1.351	0.284	4	0.085	0.985
Armatimonadetes	2	8.994	0.002**	2	0.392	0.681	4	0.159	0.955
Bacteroidetes	2	0.101	0.904	2	0.893	0.426	4	0.258	0.900
Chloroflexi	2	2.100	0.151	2	5.644	0.012*	4	0.544	0.705
Ochrophyta	2	0.398	0.677	2	0.312	0.735	4	0.213	0.928
Cyanobacteria	2	1.564	0.236	2	4.724	0.024*	4	0.584	0.678
Dependentiae	2	2.469	0.112	2	0.990	0.390	4	0.733	0.581
Firmicutes	2	0.663	0.527	2	0.399	0.676	4	0.368	0.828
Fusobacteria	2	4.214	0.031*	2	24.164	<0.001***	4	3.709	0.022*
Gemmatimonadetes	2	2.624	0.099	2	3.541	0.0505	4	0.832	0.521
Planctomycetes	2	7.991	0.003**	2	2.682	0.095	4	0.743	0.574
Proteobacteria	2	0.167	0.847	2	0.340	0.716	4	0.374	0.824
Spirochaetes	2	0.043	0.957	2	0.565	0.578	4	0.630	0.647
Verrucomicrobia	2	1.057	0.368	2	1.858	0.184	4	0.806	0.537
WPS-2	2	4.048	0.035*	2	6.939	0.006**	4	2.741	0.060
Family in Bacteroidetes									
AKYH767	2	6.231	0.008**	2	0.6251	0.546	4	0.6263	0.649
Chitinophagaceae	2	0.633	0.542	2	1.3487	0.284	4	0.152	0.959
Crocinitomicaceae	2	3.144	0.067	2	5.140	0.017*	4	0.830	0.523
env.OPS17	2	2.073	0.154	2	0.139	0.871	4	0.0511	0.994
Flavobacteriaceae	2	2.003	0.163	2	0.310	0.736	4	1.0736	0.3985
Microscillaceae	2	1.522	0.244	2	3.381	0.056	4	0.599	0.667
NS11	2	2.992	0.075	2	0.409	0.670	4	0.950	0.457
NS9	2	3.556	0.049*	2	0.528	0.598	4	0.509	0.729
Saprospiraceae	2	0.626	0.545	2	2.392	0.119	4	1.846	0.163
Spirosomaceae	2	0.299	0.744	2	0.777	0.474	4	1.379	0.280
Family within Proteobacteria									
Burkholderiaceae	2	1.105	0.352	2	0.094	0.909	4	0.545	0.704
Caulobacteraceae	2	2.296	0.129	2	3.481	0.052	4	0.438	0.779
Chromobacteriaceae	2	1.403	0.271	2	2.626	0.099	4	0.218	0.924
Pseudomonadaceae	2	4.549	0.025*	2	2.115	0.149	4	0.647	0.635
Reyranellaceae	2	1.051	0.370	2	4.368	0.028*	4	0.502	0.734
Rhizobiaceae	2	0.564	0.578	2	0.122	0.885	4	0.235	0.914
Rhodobacteraceae	2	2.269	0.132	2	0.399	0.676	4	1.239	0.329
Rhodocyclaceae	2	0.220	0.804	2	11.724	<0.001***	4	0.233	0.915
Rickettsiaceae	2	0.494	0.618	2	5.042	0.018*	4	0.093	0.983
Sphingomonadaceae	2	0.900	0.424	2	0.159	0.853	4	0.236	0.914
Xanthobacteraceae	2	0.279	0.759	2	4.775	0.021*	4	0.924	0.471
Family within Planctomycetes									
Gemmataceae	2	1.033	0.376	2	2.012	0.162	4	0.177	0.947
Phycisphaeraceae	2	5.675	0.012*	2	0.936	0.410	4	1.760	0.180

Pirellulaceae	2	3.134	0.067	2	4.172	0.032*	4	1.073	0.398
Rubinisphaeraceae	2	4.871	0.020*	2	0.191	0.827	4	0.054	0.994
Schlesneriaceae	2	8.785	0.0021**	2	0.323	0.728	4	0.255	0.902
Tepidisphaeraceae	2	2.517	0.108	2	0.517	0.605	4	0.378	0.820